# DESIGN AND DEVELOPMENT OF SMART WEIGHING LYSIMETER FOR EVAPOTRANSPIRATION STUDIES

**By**

DHAKSHINA DEVADASAN (2021-02-001)

ASHIKA N (2021-02-013)

AKSA ELIZABETH JOSE (2021-02-015)


**DEPARTMENT OF IRRIGATION AND DRAINAGE ENGINEERING**

**KELAPPAJI COLLEGE OF AGRICULTURAL ENGINEERING AND FOOD TECHNOLOGY**

**TAVANUR-679573, MALAPPURAM**

**KERALA, INDIA**

**2025**

# DESIGN AND DEVELOPMENT OF SMART WEIGHING LYSIMETER FOR EVAPOTRANSPIRATION STUDIES

**BY**

**DHAKSHINA DEVADASAN (2021-02-001)**

**ASHIKA N (2021-02-013)**

**AKSA ELIZABETH JOSE (2021-02-015)**

**PROJECT REPORT**

Submitted in partial fulfilment of the requirement for the degree of

***BACHELOR OF TECHNOLOGY IN AGRICULTURAL ENGINEERING***

**Faculty of Agricultural Engineering and Technology**


**Kerala Agricultural University**

**DEPARTMENT OF IRRIGATION AND DRAINAGE ENGINEERING**

**KELAPPAJI COLLEGE OF AGRICULTURAL ENGINEERING AND FOOD TECHNOLOGY**

**Tavanur-679573, Malappuram**

**Kerala, India**

**2025**

## DECLARATION

We, hereby declare that this thesis entitled "**DESIGN AND DEVELOPMENT OF SMART WEIGHING LYSIMETER FOR EVAPOTRANSPIRATION STUDIES**" is a bonafide record of research work done by us concerning the research work and the thesis has not previously formed the basis for the award to us of any degree, diploma, associateship, fellowship or other similar title of any other university or society.

Date: 04/06/2025

Place: Tavanur

Dhakshina Devadasan

(2021-02-001)

Ashika N

(2021-02-013)

Aksa Elizabeth Jose

(2021-02-015)

## CERTIFICATE

This is to certify that the project entitled **"DESIGN AND DEVELOPMENT OF SMART WEIGHING LYSIMETER FOR EVAPOTRANSPIRATION STUDIES"** is a record of the project work done jointly by **Ms. DHAKSHINA DEVADASAN (2021-02-001), Ms. ASHIKA N (2021-02-013), Ms. AKSA ELIZABETH JOSE (2021-02-015)** under my guidance and supervision and that it has not been previously formed the basis for the award of any degree, diploma, fellowship or associateship or other similar title of any other university or society to them.

Place: Tavanur

Date: 04/06/2025

**Guide**

Dr. REMA K.P

Professor and Head

Dept. of IDE

KCAEFT, Tavanur

**Co-Guide**

Dr. BOWLEKAR ADWAIT PRAKASH

Assistant Professor (C)

Dept. of SWCE

KCAEFT, Tavanur

## *ACKNOWLEDGEMENT*

*First and foremost, we extend our heartfelt gratitude to the Almighty for granting us the strength, patience, and determination to successfully complete this project.*

*We are deeply honoured to express our sincere thanks to our respected guide,* ***Dr. Rema K.P.,*** *Professor and Head, Department of Irrigation and Drainage Engineering, KCAEFT, Tavanur, for her constant encouragement, expert guidance, and valuable suggestions throughout the course of this work. Her insights and support were crucial in shaping and executing the project effectively.*

*We would like to express our sincere gratitude to our co-guide****, Dr. Bowlekar Adwait Prakash,*** *Assistant Professor (C), Department of Soil and Water Conservation Engineering, KCAEFT, Tavanur, for his dedicated mentorship, technical guidance, and continuous support throughout the project period.*

*We gratefully acknowledge the support and encouragement of* ***Dr. Jayan P. R.,*** *Dean of Faculty and Professor & Head, Department of Farm Machinery and Power Engineering, KCAEFT, Tavanur, for his valuable inputs and academic inspiration during our study.*

*We would also like to extend our heartfelt thanks to* ***Er. Siddhram****, Young Professional (Agri. Engg) PFDC Tavanur, for his technical assistance and involvement, which greatly contributed to the practical aspects of the project.*

*Our special thanks to* ***Mr. Dhanesh****,* ***Mr. Akash****,* ***Mr. Jithesh****, and* ***Mr. Abhijith****, whose efforts in the fabrication of the lysimeter and the laying of the drip irrigation system were indispensable to the successful execution of our work.*

*Lastly, we express our gratitude to all those who have supported us directly or indirectly in the successful completion of this project. Their help, though not mentioned individually, is truly appreciated and acknowledged with heartfelt thanks.*

***Dhakshina Devadasan***

***Ashika N***

***Aksa Elizabeth Jose***

*DEDICATED TO OUR AGRICULTURAL ENGINEERING PROFESSION*

**TABLE OF CONTENTS**

# LIST OF TABLES

# LIST OF PLATES

# LIST OF FIGURES

## SYMBOLS AND ABBREVIATIONS

| | | |
|---|---|---|
| CWR | : | Crop Water Requirement |
| % | : | Percentage |
| & | : | And |
| = | : | Equal To |
| ◦ | : | Degree |
| ◦C | : | Degree Celsius |
| Atm | : | Atmosphere |
| Cu | : | Consumptive use |
| Dept | : | Department |
| ET | : | Evapotranspiration |
| *et al* | : | And others |
| $ET_C$ | : | Crop evapotranspiration |
| $ET_O$ | : | Reference Evapotranspiration |
| $K_C$ | : | Crop Coefficient |
| FAO | : | Food and Agricultural Organisation |
| Fig | : | Figure |
| Kg | : | Kilogram |
| H | : | Hour |
| J. | : | Journal |
| KAU | : | Kerala Agricultural University |
| KCAE&FT | : | Kelappaji College of Agricultural Engineering and Food Technology |

| | | |
|---|---|---|
| L | : | Litre |
| m | : | Metre |
| cm | : | Centi metre |
| mm | : | Milli metre |
| $m^2$ | : | Square metre |
| $m^3$ | : | Cubic metre |
| PVC | : | Poly vinyl chloride |
| LDPE | : | Low density polyethylene |
| $R^2$ | : | Coefficient of determination |
| RH | : | Relative humidity |
| RMSE | : | Root mean square error |
| s | : | Second |
| I2C | : | Inter integrated circuit |
| RTC | : | Real-Time Clock |
| GP | : | Galavanized Plain |
| LCD | : | Liquid-Crystal Display |

# *Introduction*

# CHAPTER I

# INTRODUCTION

Water isn't just limited; it is a natural resource that serves as the lifeblood of human existence and socio-economic development. Agriculture worldwide accounts for about 69-70% of total renewable freshwater withdrawals, making it the most water-intensive human activity (Du Plessis, 2017). In India, more than 80% of total water consumption is attributed to irrigation. Compared to non-irrigated systems, which often fail to meet crop requirements as it depends on seasonal rainfall which is highly erratic, irrigation has boosted productivity in most regions (Jain *et al*., 2019).

With growing pressure from urban and industrial sectors, the share of water available for agriculture is steadily declining. This highlights the urgent need for scientific water management and precision irrigation to ensure food security, maintain soil health, and promote long-term agricultural sustainability. To achieve above 70% efficiency levels within any irrigation system, water should be applied in the right amounts at the appropriate times as per the specific ET needs of the crops. This is achieved by irrigation scheduling, determining when and how much water to apply, as per real-time measures or estimates on climate demand ($ET_0$) and soil moisture status (Rahil and Qanadillo, 2015).

Evapotranspiration is the most important part of the hydrological cycle, returning most of the precipitation that falls on land surface areas back into the atmosphere. ET utilizes nearly 60% of the annual precipitation landing on the earth (Irmak, 2009). Therefore, considering crop evapotranspiration requirements plays a significant role in irrigation planning, water-resource management, and environmental assessments. The accurate estimation of evapotranspiration is regarded as one of the most important input parameters in planning and designing an irrigation system, and accurately determining the spatial distribution of ET is key to achieving sustainable agricultural development.

Evapotranspiration requirements at critical growth stages of the crop are essential in deciding when to irrigate the crops. Transpiration may be brought to a halt once the value of evapotranspiration exceeds the plant water availability due to precipitation or irrigation. So, an accurate estimation of ET, together with the knowledge of

precipitation amounts and soil moisture storage capacity, can give insight into the correct amount of water to be applied through irrigation (Villalobos *et al*., 2017).

Crop evapotranspiration ($ET_c$) is the most important element in terms of water balance in arid and semi-arid zones and is a governing parameter for efficient irrigation scheduling and increasing water use efficiency in irrigated agriculture. $ET_c$ differs from reference crop evapotranspiration ($ET_0$) since ground cover, canopy properties, and aerodynamic resistance differ from those of grass. Actual water uptake rate of the crop from the soil in relation to crop evapotranspiration ($ET_c$) depends on whether the available water in the soil is sufficient or the crop will undergo some degree of stress due to water deficit (Rana *et al*., 1994).

Evapotranspiration has a linear relationship with climate for the majority of crops when a crop coefficient (Kc) is used, this coefficient being defined as $K_c = ET_c / ET_0$. $K_c$ refers to the evapotranspiration of a healthy crop grown over large areas under optimum water and fertility conditions, achieving its maximum production potential under the local environmental conditions (Allen *et al*.,1998). It encompasses the physical and physiological differences between the crop and the reference grass, which ultimately integrates the differences between the evaporation and transpiration of the field crops and that of the reference grass surface. Factors affecting $K_c$ are the type of crop, crop growth stage, climate, and soil moisture. The crop coefficient is, therefore, most commonly represented as a function of time. Hence, most researchers have reported $K_c$ values as a function of days after transplanting, which denote $K_c$ for different development stages of the crop (Guerra *et al*., 2016).

Lysimeters are specialized instruments designed to isolate a soil column in order to study water inflow and outflow, making them invaluable tools for understanding crop water use and soil water balance. The earliest documented use of lysimeters dates back to 1668 in France, when La Hire employed lead containers filled with soil to observe water loss (Aboukhaled *et al*., 1982). By accurately replicating field conditions, lysimeters provide reliable data on water balance components such as evapotranspiration, drainage, and soil moisture changes. This ability makes them essential in investigating plant-water relationships and managing irrigation effectively (Meissner *et al*., 2010).

Lysimeters come in various designs and sizes depending on research objectives and resource availability. Common shapes include rectangular, circular, and square forms, while micro-lysimeters with very small surface areas are used for direct measurement of soil surface evaporation (Tyagi *et al*., 2000; Yang *et al*., 2003; Schneider *et al*., 1998; Jiménez-Carvajal *et al*., 2017). These diverse designs allow researchers to study water and solute dynamics in the soil profile with precision (Marek *et al*., 2006).

The accuracy of measurements from lysimeters depends heavily on their proper installation, operation, and maintenance (Malone *et al*., 2000). By isolating a specific soil volume and measuring water inputs and outputs, lysimeters can simulate natural field conditions such as soil moisture distribution, root density, and plant height, though challenges remain in perfectly replicating deeper soil moisture dynamics (Schneider *et al*., 1998).

Among the different types, weighing lysimeters are widely regarded as one of the most accurate tools for measuring crop evapotranspiration ($ET_c$). These devices determine changes in soil moisture by continuously or intermittently measuring the weight of the soil-plant system over time. The fluctuations in weight, combined with records of precipitation, irrigation, and drainage, allow precise calculation of mean crop $ET_c$ for given periods (Burman *et al*., 1983). Early classifications of weighing lysimeters divided them into intermittent and continuous types, distinguished mainly by the time interval between weight measurements. Continuous weighing lysimeters provide high-frequency data and superior accuracy but involve higher installation costs, require skilled personnel, and need permanent field setups, which limit their portability and broader application (Howell *et al*., 1991).

Weighing lysimeters are extensively used to monitor crop water use at different growth stages and to develop localized crop coefficients that support irrigation scheduling and water management strategies. Their precise measurement capabilities make them a gold standard, despite the rise of indirect methods which are faster but generally less direct (Allen *et al*., 1991; Kumari & Srivastava, 2020). Historically, weighing lysimeters relied on mechanical systems that required regular maintenance. However, advances in electronic components, including load cells and data loggers,

have enabled the development of smart weighing lysimeters. These modern instruments offer improved accuracy, reduced cost, and lower maintenance demands, making them more accessible for widespread research and application (Farzaneh Zardoshti *et al*., 2018).

Therefore, this study proposes to design and develop a continuously weighing lysimeter to determine actual evapotranspiration. The primary objectives of the study are:

1. To design and develop a smart weighing lysimeter.
2. To determine the actual evapotranspiration of *Amaranthus dubius* inside a polyhouse using the developed smart weighing lysimeter.
3. To estimate crop coefficient of *Amaranthus dubius*.

# *Review of literature*

# CHAPTER II

# REVIEW OF LITERATURE

This chapter critically reviews the previous research work related to the present study.

## 2.1 SIGNIFICANCE OF EVAPOTRANSPIRATION (ET)

Reference evapotranspiration ($ET_0$) serves as a critical climatic parameter in estimating crop water needs and planning irrigation. Early lysimetric work by Van Bavel and Wilson (1952) and Penman (1956) laid the foundation for understanding $ET_0$ by relating it directly to climate. Monteith (1959) refined Penman's approach by integrating stomatal and surface resistance, improving accuracy under varying conditions.

Field studies in the 1950s and 60s further illuminated the roles of crop height, ground cover, and growth stage on ET rates (Marlatt, 1961; Tanner and Lemon, 1962; Viets, 1962). Haise *et al*. (1963) and Dreibelbis and Amerman (1964) emphasized the effects of surface albedo and roughness, while Ekern (1965) showed how stomatal regulation alters ET across crops.

Hargreaves (1989, 1994) proposed simplified $ET_0$ models suited for arid and semi-arid regions, helping standardize $ET_0$ as a climatic demand independent of crop and soil type. Allen *et al*. (1994, 1998) then formalized the FAO Penman-Monteith method using a hypothetical grass reference, enabling global consistency in $ET_0$ estimation.

Later evaluations (Tabari, 2010; Kumar *et al*., 2012) showed that empirical models like Hargreaves–Samani and Priestley–Taylor perform reliably in data-sparse regions when calibrated locally. Talebmorad *et al*. (2021) linked $ET_0$ trends to climate change in semi-arid Iran. In India, Niranjan and Nandagiri (2023) and Drema *et al*. (2024) developed regional $ET_0$ datasets and maps, supporting localized water management and drought adaptation.

### 2.1.1 Reference crop evapotranspiration ($ET_0$)

$ET_0$ represents the atmospheric demand for water vapor and serves as a fundamental baseline for estimating crop water requirements. Essentially, $ET_0$ defines the amount of water that a standardized reference surface, commonly a well-watered grass of specific height and surface properties would lose through evaporation and transpiration under given climatic conditions. Allen *et al*. (1994) formalized this reference as grass of 0.12 meters height, with a surface resistance of 70 s $m^{-1}$ and an albedo (reflectivity) of 0.23. This standardization allows the derivation of crop-specific evapotranspiration by applying crop coefficients ($K_C$), which adjust $ET_0$ values to match the water use characteristics of various plants.

The importance of this standardized $ET_0$ was further emphasized by Hargreaves (1994), who demonstrated that aligning all ET equations to this reference surface significantly improves their comparability and robustness across different climatic zones. This harmonization also underpins advanced remote sensing techniques such as the Surface Energy Balance Algorithm for Land (SEBAL), which estimates ET over large areas using satellite data.

Allen *et al*. (1998) reinforced that $ET_0$ values are independent of soil type and crop species, ensuring that measurements and estimations remain comparable regardless of the local environment. However, when full meteorological data are unavailable, simplified empirical models are often used. Tabari (2010) evaluated several reduced-data $ET_0$ models and found that local calibration based on climate context can reduce estimation errors by up to 35% compared to the FAO-56 Penman–Monteith standard. Specifically, the Turc equation performed better in colder, arid climates, while the Hargreaves–Samani model was more accurate in warmer and semi-arid regions.

Kumar *et al*. (2012) reaffirmed the FAO-56 Penman–Monteith method as the gold standard for $ET_0$ estimation where comprehensive weather data (solar radiation, temperature, humidity, wind speed) is available. Nevertheless, for regions with sparse data, locally calibrated simpler methods like Hargreaves or Priestley–Taylor can provide practical alternatives.

Climate projections, such as those for Iran analyzed by Talebmorad *et al*. (2021), indicate that $ET_0$ is likely to increase due to warming temperatures by about 4% by mid-century (2049) and 12% by the end of the century (2099). These increases underscore the urgency for adaptive irrigation scheduling to maintain water use efficiency under changing climatic conditions.

Operational applications of $ET_0$ include gridded data products, which are now increasingly used for regional drought early warning systems, exemplified by efforts in Karnataka (Niranjan & Nandagiri, 2023), and for fine-tuning rice irrigation management in Arunachal Pradesh (Drema *et al*., 2024). Such implementations demonstrate $ET_0$'s pivotal role in both research and practical water resource management.

### 2.1.2 Factors affecting evapotranspiration (ET)

Evapotranspiration (ET) encompasses the combined processes of water evaporation from the soil surface and transpiration through plant leaves. It is influenced by a complex interplay of biophysical plant characteristics and environmental factors governing the exchange of water vapor between the land surface and atmosphere. The following sub-sections describe the main factors affecting ET in detail:

#### *2.1.2.1 Plant species*

Different plant species regulate water loss in distinctive ways due to their physiological and anatomical adaptations. For example, well-watered crops such as alfalfa and grass can transpire approximately 5 mm per day, while plants employing Crassulacean Acid Metabolism (CAM), like pineapple, exhibit much lower daily ET around 2 mm. This difference reflects the water-use efficiency mechanisms adapted to arid environments, enabling CAM plants to conserve water by opening stomata primarily at night (Van Bavel & Wilson, 1952; Ekern, 1965).

#### *2.1.2.2 Surface albedo*

Surface albedo, the proportion of sunlight reflected by the surface, significantly impacts ET by altering the available energy for evaporation. A 15% increase in surface reflectance can reduce ET by 10–15%, as less solar radiation is absorbed to drive evaporation (Penman, 1956). Vegetation canopies generally reflect 20–30% of

incoming radiation, while bare soil surfaces reflect less, typically between 11–23% (Monteith, 1959; Haise *et al*., 1963). These differences influence the energy balance and thus the evaporative demand from the surface.

#### *2.1.2.3 Plant cover*

The extent of plant cover is directly correlated with ET rates. Research indicates that ET increases by approximately 0.1 mm per day for every 10% increase in canopy cover until around 50%, beyond which ET approaches levels typical of a fully covered surface (Marlatt, 1961; Tanner & Lemon, 1962). This relationship highlights the significant role of vegetation density in regulating water loss.

#### *2.1.2.4 Plant population density and row spacing*

Planting density and spatial arrangement affect transpiration by modifying leaf area and shading effects. For example, increasing corn density from 5,000 to 10,000 plants per acre raised ET from 4.0 to 5.5 mm per day (Tanner *et al*., 1960). Denser plantings result in greater leaf area, enhancing transpiration and shading soil surfaces, thereby reducing soil evaporation.

#### *2.1.2.5 Plant height*

The height of the plant canopy influences ET by affecting solar radiation interception and the microclimate around the plants. Taller canopies absorb more sensible heat and can increase ET by 5–10%, especially under high temperature and isolated plant conditions (Viets, 1962).

#### *2.1.2.6 Root depth*

Root system depth plays a critical role in ET by determining the soil moisture accessible to plants. Deep-rooted species can access more soil water and maintain higher transpiration rates during peak demand periods. For instance, deep-rooted grasses have been shown to consume approximately 90 mm more water annually than shallow-rooted varieties, which translates to roughly an additional 1.5 mm per day at peak usage (Dreibelbis & Amerman, 1964).

#### *2.1.2.7 Growth stage*

ET varies considerably across the growth stages of a plant. Early in the season, ET is low (~2 mm $d^{-1}$) due to limited leaf area and undeveloped roots. As the plant matures, ET reaches its peak (~6 mm $d^{-1}$) because of maximal leaf area and metabolic activity. ET then declines (~3 mm $d^{-1}$) during the senescence phase as leaves age and plants produce seed heads (Lemon *et al*., 1957; Fritschen & Van Bavel, 1964).

#### *2.1.2.8 Management practices*

From an agricultural management perspective, ET can be reduced by lowering canopy cover, selecting short-season or succulent species, or manipulating stomatal conductance. However, attempts to induce partial stomatal closure to conserve water have yielded inconsistent results (Gale, 1961; Zelitch, 1964). A thorough understanding of these factors is essential for optimizing irrigation scheduling and improving overall water use efficiency in agricultural systems.

### 2.1.3 Polyhouse micro-climate and ET

Polyhouse or protected cultivation systems modify the surrounding micro-climate in ways that consistently suppress reference evapotranspiration ($ET_0$), generally by 18–35%. This suppression primarily arises from elevated humidity levels and reduced vapour pressure deficits (VPD), which lower the atmospheric demand for water vapor.

Studies utilizing computational fluid dynamics (CFD) models, such as the one by Gupta *et al*. (2020), have identified critical design parameters influencing micro-climate control within polyhouses. Ventilation openings and fan layouts are the principal levers controlling temperature and humidity, with validated models accurately predicting internal temperature within ±1.2 °C and relative humidity within ±6%. This precision is vital for optimizing irrigation and crop management schedules.

Sensor network deployments, such as the ZigBee-based system used by Kolapkar and Sayyad (2020) in a 400 $m^2$ greenhouse, revealed that vapor pressure deficit varies spatially within protected structures. Their research showed that leeward areas experienced higher VPD, causing yield variations of up to ±9%. Importantly, they demonstrated that node-based VPD-triggered irrigation systems could reduce water use by approximately 12%, highlighting the potential for precision irrigation in polyhouses.

Long-term field data from Odisha (Santosh, 2021) confirmed that $ET_0$ within polyhouses is 25–35% lower than open-field conditions, supporting recommendations to reduce the crop coefficient ($K_C$) by approximately 30% (multiplying by 0.70) for naturally ventilated structures. Similar findings from South India (Challa *et al*., 2022) showed $ET_0$ reductions of 24% in winter and 18% in summer, coupled with a 27% increase in cucumber yields and a substantial improvement in water use efficiency (from 6.2 to 9.1 kg $m^{-3}$).

In Egypt, Abd El-Bary *et al*. (2022) combined 60 µm polyethylene tunnels with subsurface drip irrigation, resulting in a 46% yield increase and a 56% improvement in water use efficiency for tomatoes, illustrating the synergistic effects of micro-climate control and precise irrigation.

Research from Gujarat (Sojitra *et al*., 2023) confirmed a 22% decrease in $ET_0$ inside polyhouses compared to open fields, and advised scaling down drip irrigation schedules by a factor of 0.75 in semi-arid regions to match the reduced atmospheric demand.

In summary, polyhouses reduce evaporative demand by increasing humidity and reducing wind effects, which lowers $ET_0$ and irrigation requirements. These systems also often enhance crop yields and water productivity. However, to fully realize these benefits, irrigation scheduling must be adapted to the altered micro-climate conditions inside the protected environment, emphasizing the need for localized management strategies.

## 2.2 WEIGHING LYSIMETER

Kebede *et al*. (2024) developed a low-cost manual weighing lysimeter for field use in Ethiopia. Built with accessible materials and a manual hydraulic lift, it accurately measured crop water use through mass change. Despite lacking automation, its affordability and simplicity made it ideal for smallholder systems in data-scarce areas. Static calibration confirmed its reliability for estimating evapotranspiration (ET) and crop water requirements.

Gao *et al*. (2025) reviewed lysimeter advancements in China, detailing a shift from manual systems to automated, sensor-integrated units enhanced with artificial

intelligence (AI) and machine learning (ML) for predictive irrigation and ET modelling. The study highlighted the transformative role of intelligent lysimeters in sustainable water management.

Stockle *et al*. (2025) compared ET estimation models—CropSyst-W, EEFlux, and OpenET—against data from four precision weighing lysimeters in Texas. CropSyst-W showed the best agreement with lysimeter data (Willmott index = 0.93, NRMSD = 0.31), validating the importance of weighing lysimeters as benchmarks for irrigation model accuracy.

### 2.2.1 Smart weighing lysimeter

Nicolás Cuevas *et al*. (2020) introduced a lightweight (≈ 6 kg), removable lysimeter for horticulture, built with three 100 kg load cells and modular PVC. It achieved high precision ($R^2 = 0.999$, RMSE ± 12 g) and was cost-effective (€180). Field ET tracking for lettuce was within 5% of reference lysimeters, supporting scalable deployment and student use.

Sagar *et al*. (2022) built a smart greenhouse lysimeter using four 150 kg load cells, HX711 amplifiers, and real-time telemetry. It logged 301 mm ET over 110 days with peak Kc of 1.06 and 0.9 Wh/day energy use. The low cost (₹59,760) and accuracy (RMSE ± 35 g) support its use in precision irrigation.

Schmidt (2022) created a portable lysimeter (0.45 × 0.45 m) for tomato pot trials using ESP32, SD storage, and Wi-Fi. It had low hysteresis (<0.03%), high accuracy (RMSE ± 8 g), and cost ₹25,700. ET tracked within 4% of gravimetric checks, enabling open-source, low-cost research in controlled environments.

Oliveira *et al*. (2022) integrated IoT and blockchain in a lysimeter system for secure soil-water monitoring, enhancing data reliability and supporting future AI-based irrigation and anomaly detection models.

Dong and Hansen (2023) built a DIY field-scale lysimeter (1.2 × 1.2 × 1.0 m) with 500 kg load cells, Arduino Mega, and solar-powered LoRa telemetry. Static calibration gave $R^2 = 0.998$, RMSE ± 90 g. Over a 60-day maize trial, the system recorded 165 mm ET, just 3% below eddy covariance, demonstrating research-grade accuracy at ₹87,000 cost.

Abhiram *et al*. (2023) developed a modular lysimeter system for climate-controlled environments with high-frequency environmental and plant monitoring. Though not AI-integrated, it supports ML-ready data generation for ET prediction, irrigation optimization, and anomaly detection.

Rajput *et al*. (2024) installed two 1 m³ lysimeters for broccoli in New Delhi to derive FAO-56 based $K_c$, $K_{cb}$, and $K_e$ values. They logged 285 mm seasonal ET with calibration RMSE ± 80 g and drift <0.03%. Applying derived coefficients in AquaCrop reduced irrigation demand by 18%, improving water productivity by ~35 mm over farmer practices.

## 2.3 COMPUTATION OF $ET_C$ USING LYSIMETERS

Ahmed (1991) conducted a comprehensive evaluation of lysimeters, comparing them to indirect methods of ET measurement. His findings affirmed that lysimeters are highly reliable, providing accurate data for calculating ET, which is critical for efficient irrigation planning. The study emphasized that while indirect methods can offer quick estimates, they often lack the precision provided by lysimeter data, especially in regions where water management is crucial. Ahmed concluded that lysimeters are essential for developing water-efficient irrigation schedules, particularly in areas with variable rainfall and unreliable meteorological data.

Pandey and Pandey (2011) focused on the application of lysimeters in various agricultural systems to assess crop ET. They found that lysimeter data offers direct measurements of ET that are more accurate compared to weather-based models, which can be influenced by inconsistencies in climate data. Their study highlighted the importance of lysimeters for precise crop water requirement calculations, which are crucial for optimizing irrigation practices. The authors recommended the use of lysimeters in regions with erratic weather patterns, as they provide the most accurate information for managing irrigation effectively.

Kumar and Kumar (2012) extended their investigation into lysimeter-based ET estimation, focusing on different crop types. They demonstrated that lysimeters are superior in measuring crop-specific water use compared to indirect estimation methods. The study showed that lysimeters provide critical insights into water requirements,

which are essential for designing water-efficient irrigation systems. Kumar and Kumar concluded that although lysimeters require more investment in terms of time and resources, they are indispensable for accurate water management, especially in areas facing water scarcity.

Doležal *et al*. (2018) conducted a study on the actual evapotranspiration ($ET_a$) of unirrigated grass using a smart field lysimeter in a warm region of the Czech Republic. Their research demonstrated that small smart lysimeters are effective tools for high-quality research on low and dense crops. The study found that the FAO 56 method could reasonably estimate reference crop $ET_0$ on non- or mildly stressed sites. Additionally, the relationship between measured $ET_a$ and calculated $ET_0$ was influenced by soil water content and suction at 5 cm depth, with the $ET_a/ET_0$ ratio being approximately 85% and canopy surface resistance around 250 s $m^{-2}$ when the grass was not under water stress. These findings underscore the importance of lysimeters in accurately assessing crop water use, which is crucial for optimizing irrigation practices in water-limited environments.

Meena *et al*. (2021) explored lysimeter-based measurements of ET under different irrigation methods, including drip and sprinkler systems. They found that lysimeter data offered a more accurate reflection of crop water use than models based on climatic data, which can be less reliable under changing irrigation conditions. The study highlighted that lysimeters provide detailed, site-specific information on crop water requirements, which is essential for tailoring irrigation strategies to local conditions. Meena *et al*. concluded that lysimeter-based ET measurements are vital for enhancing water use efficiency and developing sustainable irrigation practices.

Schrader *et al*. (2023) examined lysimeter-based ET measurements in various climatic regions, emphasizing their importance in developing region-specific irrigation strategies. They found that lysimeters provide accurate data that are crucial for tailoring irrigation practices to local conditions. Their research highlighted that lysimeter data can help farmers in areas with limited meteorological data to make better irrigation decisions. Schrader *et al*. concluded that lysimeters are essential for improving water management practices in diverse climates, particularly where reliable meteorological data are scarce.

Shi *et al*. (2023) conducted a detailed study on lysimeter-based evapotranspiration (ET) measurements in controlled greenhouse environments. Their research compared the accuracy of lysimeter data with several commonly used ET estimation models, including Penman–Monteith, Hargreaves–Samani, pan evaporation, and artificial neural networks. The results showed that lysimeters provided more precise and reliable ET values, serving as a benchmark for evaluating other models. The study highlighted the significance of lysimeter data in capturing the spatial and temporal variability of ET, which is essential for optimizing irrigation scheduling and improving water-use efficiency. The findings support the use of lysimeters in designing location-specific irrigation strategies, particularly in climates where model-based estimations may lack accuracy.

Lysimeters provide the most accurate and reliable method for estimating evapotranspiration, which is essential for developing effective irrigation strategies and managing water resources efficiently. The reviewed studies consistently highlight the advantages of lysimeters over indirect methods, particularly in regions where precise water management is critical. Lysimeter-based data help optimize irrigation schedules, improve water use efficiency, and enhance crop productivity, making them invaluable tools in agricultural systems worldwide. While they require more investment and effort compared to other methods, the accuracy and site-specific data they provide are crucial for sustainable agricultural water management, particularly in water-scarce or variable climatic regions.

## 2.4 DEVELOPMENT OF CROP COEFFICIENT CURVES

Accurate estimation of crop evapotranspiration ($ET_C$) is critical for irrigation scheduling and water resource management. The use of lysimeters, particularly weighing lysimeters, has been the most reliable method for direct measurement of $ET_C$, thereby allowing the development of precise crop coefficient ($K_C$) curves. Weighing lysimeters function by continuously recording the weight changes in a soil column containing a crop, which directly corresponds to water loss through evapotranspiration. These instruments offer high temporal resolution and accuracy (Pereira *et al*., 2021).

Sagar *et al*. (2022) developed a portable smart weighing lysimeter to determine crop coefficient values for chrysanthemum under greenhouse conditions at the Indian

Agricultural Research Institute. The study reported Kc values of 0.43 (initial), 1.27 (mid-season), and 0.67 (end season) for 2019–20, and 0.38, 1.25, and 0.59 for 2020–21 respectively, which closely matched the FAO-56 standard. Similarly, Reddy *et al*. (2023) employed a weighing type lysimeter for tomatoes grown in the Raichur region, Karnataka. The observed $K_C$ values during the rabi season were 0.38 (initial), 0.64 (development), 1.12 (mid-season), and 0.66 (late season). Their findings reinforced the variability in $K_C$ values with seasons and agro-climatic conditions.

Kashyap and Panda (2001) had earlier noted that crop coefficients are not universal and require regional calibration using lysimetric methods, especially for crops like rice and maize. In line with this, Abedinpour (2015) reported that the $K_C$ values for maize under semi-arid conditions ranged from 0.40–0.60 (initial), 0.70–0.80 (development), 1.10–1.21 (mid-season), and 0.50–0.65 (late season). Sarma and Bharadwaj (2020) studied rapeseed using a weighing lysimeter and different $ET_0$ models. The Penman-Monteith model yielded $K_C$ values of 0.83, 1.20, and 0.65 for initial, mid, and late stages respectively. The study concluded that FAO-recommended $K_C$ values were inadequate for the Assam region.

Toyin *et al*. (2015) conducted a greenhouse study at the Federal University of Technology, Akure, Nigeria, to determine the evapotranspiration and crop coefficient ($K_C$) of *Amaranthus cruentus* using weighing lysimeters. The experiment revealed that crop evapotranspiration ($ET_C$) increased progressively with plant growth, ranging from 4.5 mm/week during the first week after planting to 14.3 mm/week in the seventh week. Correspondingly, the $K_C$ values increased from 0.15 at emergence to 0.36 at maturity, indicating clear stage-wise variation in crop water use. The study demonstrated that weighing lysimeters are highly effective in precisely quantifying water use for leafy vegetables under controlled conditions, making them valuable tools for developing accurate crop coefficient curves. Studies by López-Urrea *et al*. (2021) and Gonzalez *et al*. (2023) further emphasized that climate, soil texture, cultivar, and management practices strongly influence $K_c$, necessitating localized calibration through lysimetric observations. Thus, it is evident that weighing lysimeters play a pivotal role in accurately determining crop coefficients, which are critical inputs for modelling irrigation water requirements in precision agriculture.

## 2.5 ESTIMATION OF ET USING CROPWAT MODEL

The CROPWAT model, developed by FAO, is widely used for estimating reference evapotranspiration ($ET_0$), crop evapotranspiration ($ET_C$), and irrigation requirements using the Penman–Monteith method (Allen *et al*., 1998). Its user-friendly interface and ability to simulate crop water needs across growth stages make it valuable for irrigation planning and water resource management (Smith, 1992; George *et al*., 2000; Feng *et al*., 2007).

Despite its strengths, CROPWAT's accuracy declines when default crop coefficients ($K_C$) are used without local calibration. Studies in Ukraine (Vozhehova *et al*., 2018) and Kerala (Surendran *et al*., 2015) revealed discrepancies of up to 46% in ET and 89% in irrigation requirements due to non-localized $K_C$ values. Similar concerns were raised by Romashchenko *et al*. (2016), Zhuravlev (2016), and Valipour *et al*. (2017), who advocated for region-specific $K_c$ adjustments and, in some cases, alternative ET models better suited to specific climates.

Nevertheless, CROPWAT remains a practical and accessible tool, especially when complemented by field data. Madhavi (2017) confirmed its utility in both open field and polyhouse environments, highlighting the importance of local calibration for accurate ET estimation.

# *Materials and methods*

# CHAPTER III

# MATERIALS AND METHODS

This chapter deals with the materials used and methodology adopted to fulfill the objectives of the study. It includes the details of the fabrication of smart weighing lysimeter using load cells, signal amplifiers, and an Arduino microcontroller to measure actual evapotranspiration ($ET_C$) throughout the crop's lifecycle. This chapter also includes methodology adopted for determination of $ET_0$ and $ET_c$, CROPWAT model for computation of $ET_0$ and development of crop coefficient values for *Amaranthus dubius.*

## 3.1 DESCRIPTION OF THE STUDY AREA

The experimental site was located at a geographical coordinate of 10°51'18" N latitude and 75°59'11" E longitude, with an elevation of approximately 8.54 meters above mean sea level. The field investigation was carried out within a naturally ventilated polyhouse, situated in the research plot of the Department of Irrigation and Drainage Engineering at the Kelappaji College of Agricultural Engineering and Food Technology (KCAEFT), Tavanur, Kerala.

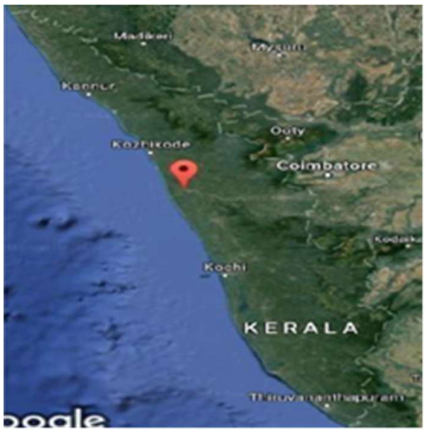


**Plate 3.1 Location of the study area**

Climatologically, the study area (Plate 3.1) lies along the transitional boundary between the northern and central agro-climatic zones of Kerala. The region predominantly receives rainfall from the southwest monsoon, which contributes to the majority of the annual precipitation. The average yearly rainfall in this area typically

ranges between 2500 mm and 2900 mm. Temperature conditions remain relatively stable throughout the year, with an average maximum temperature of around 31°C and an average minimum temperature of approximately 26°C. These climatic characteristics create a conducive setting for evaluating crop water requirements and evapotranspiration under controlled cultivation systems (Madhavi, 2017).

## 3.2 DETERMINATION OF SOIL CHARACTERSTICS

### 3.2.1 Determination of bulk density and dry density

The bulk density and dry density of the soil filled in the lysimeters were determined using the core cutter method, following standard procedures. A cylindrical core cutter was driven into the soil to extract an undisturbed sample as shown in Plate 3.2., which was then weighed (Plate 3.3), oven-dried, and reweighed to compute both bulk and dry densities

**Plate 3.2. Collection of soil sample**

**Plate 3.3. Measuring the weight of sample soil**

## 3.3 FABRICATION OF SMART WEIGHING LYSIMETER

### 3.3.1 Construction of lysimeter tank

#### *3.3.1.1 Selection and modification of the tank*

Our project commenced with the identification of a suitable container, which was a scrap tank available in the SWCE Hydraulics Laboratory. This tank was then transported to the Farm Machinery Workshop, where all fabrication work was undertaken. The tank was carefully cut and resized to the required dimensions of 110 cm length, 80 cm width, and 60 cm height, ensuring it met the experimental design criteria for housing soil and measuring weight variations accurately. This modified tank formed the structural foundation for our smart weighing lysimeter meter.

#### *3.3.1.2 Fabrication of internal support with angle iron*

To support the internal components of the lysimeter, we used angle iron sections of dimensions 50 mm × 50 mm × 6 mm. These angle iron pieces were cut and securely installed horizontally inside the tank at a depth of 45 cm from the top. They served as a robust internal frame to hold the perforated sheet, upon which soil is placed. Their sturdy construction provided adequate strength to bear the weight of the overlying soil and the changes due to the water dynamics during the experiment.

#### *3.3.1.3 Installation of the sloping sheet*

Upon the angle iron framework, a Galvanized Plain (GP) sheet of 18-gauge thickness, shaped and installed in a sloping manner as given in Plate 3.4. The purpose of this sloping sheet was to facilitate the movement of percolated water towards a specific collection point, mimicking natural field drainage patterns. This design helped prevent water accumulation and enabled precise collection for analysis**.**

**Plate 3.4 Sloping sheet inside tank**

***3.3.1.4 Perforated plate for drainage***

To enable efficient water percolation, a metal sheet was fabricated by drilling 5 mm diameter holes at 5 cm intervals. This perforated plate was then placed above the sloping GP sheet. The perforations allowed water to pass through freely while supporting the soil filled above. Importantly, filtration media such as a green net and a fiber mesh of sizes 110× 80× 60 cm was used instead of gravel, as it would have added excessive weight to the structure, causing the load cell to fail. Plate 3.5 shows fabrication of perforated plate

**Plate 3.5. Fabrication of perforated plate**

### *3.3.1.5 Drainage outlet design*

A circular outlet hole of 6 mm radius was carefully drilled into one of the lengthwise sides of the tank. This outlet served as the exit point for leachate, ensuring that water collected via the slope and perforated base could be discharged or directed to a collection vessel for further analysis. This feature played a key role in maintaining steady-state conditions within the lysimeter.

### *3.3.1.6 Construction of the supporting frame*

Once the internal structure was completed, a metal frame to support the entire setup was built. This frame had overall dimensions of 110 cm length and 80 cm width,

with legs measuring 20 cm height. It elevated the tank off the ground, ensuring space for the load cell assembly and observation. The frame was made robust enough to withstand the load from the soil-filled tank.

### *3.3.1.7 Integration of the load cell assembly*

A metal stool was placed centrally on the supporting frame, and the load cell was mounted on top of this stool (Plate 3.6). This load cell is the heart of the system, enabling real-time monitoring of weight changes due to irrigation, evapotranspiration, and crop water uptake. Above the load cell, a second stool to evenly distribute the load. The modified tank was then placed on this top stool, allowing all weight fluctuations to be captured precisely by the load cell.

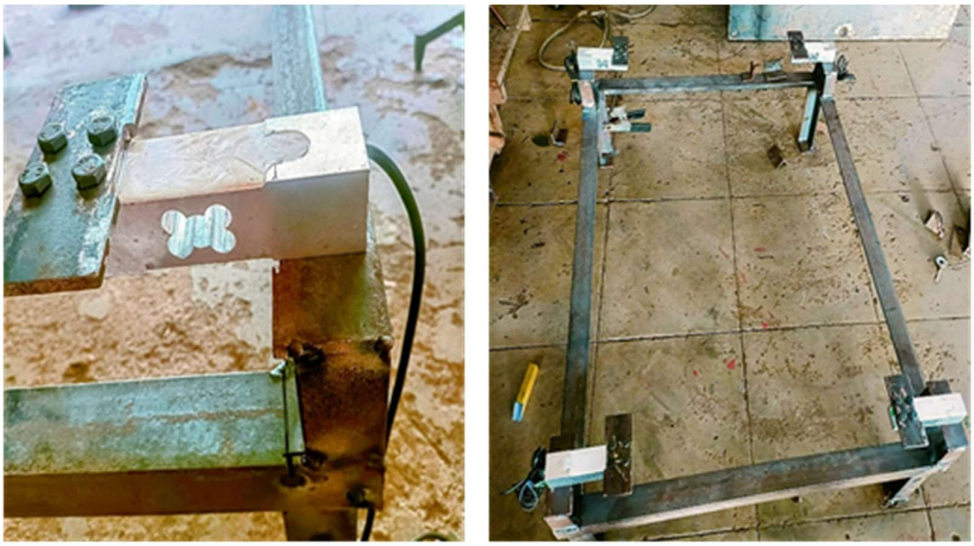

**Plate 3.6. Load cell assembly**

### *3.3.1.8 Provision for electronic components*

A tray was affixed to one of the lengthwise sides of the tank to facilitate the safe installation and housing of electronic components. This tray was designed to hold the circuitry and sensors necessary for data logging and monitoring. It ensured that all electronic parts remained elevated and protected from moisture and soil, thereby nhancing the system's durability and reliability. Plate 3.7 shows Electronic Circuit Holding Tray

**Plate 3.7 Electronic circuit holding tray**

### *3.3.1.9 Final finishing with paint*

As a finishing step, the lysimeter tank and the supporting frame were thoroughly painted to protect the metal surfaces from corrosion and weather-induced wear (Plate 3.8). This protective coating ensures long-term durability, especially when used under varying environmental conditions during field experiments. Figure 3.1 shows Three-Dimensional Representation of Lysimeter.

**Plate 3.8 Painting of the lysimeter**

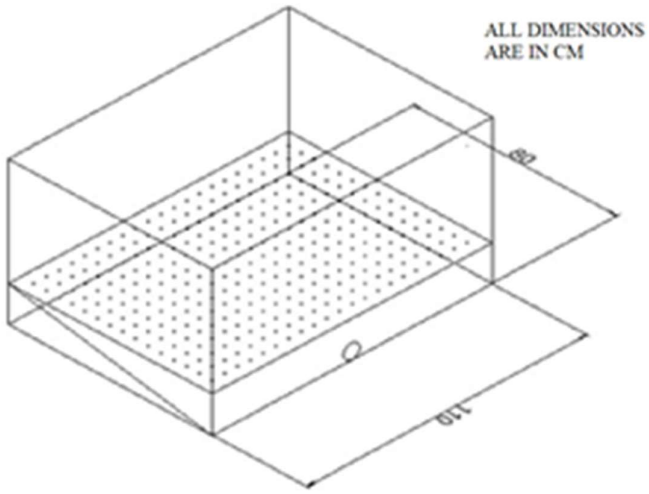


**Figure 3.1 Three-dimensional view of the lysimeter**

### 3.3.2 Assembling of load cells

To ensure precise and stable weight measurements in the smart weighing lysimeter system, a sturdy support structure for the load cells was fabricated using mild steel angle iron. As illustrated in Plate 3.9, the design comprises four vertical legs, each measuring 20 cm in height, which support a rectangular frame with dimensions corresponding to the lysimeter tank base (110 cm × 80 cm).

At each of the four corners of this rectangular frame, angle iron stools were securely welded to act as foundational platforms for the installation of load cells (refer to Plate 3.5). The load cells used were CZL-642 model strain gauge-based sensors, each with a capacity of 300 kg, procured through an online supplier. These sensors are designed to accurately capture the load applied by the lysimeter system, even under varying environmental conditions typically encountered in agricultural research settings.

An additional set of angle iron stools was strategically placed above the load cells. These served as the upper mounting base for the lysimeter tank, thereby ensuring direct, stable, and uniform load transmission from the tank to the sensors (Plate 3.10). This two-tier stool arrangement minimizes structural deflection and enhances the reliability of real-time weight readings, which are crucial for accurate evapotranspiration estimation.

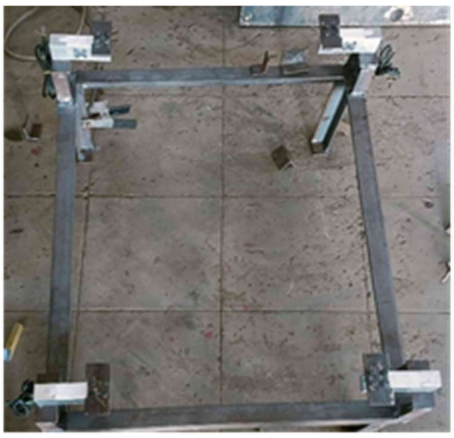

**Plate 3.9 Assembling of load cells**

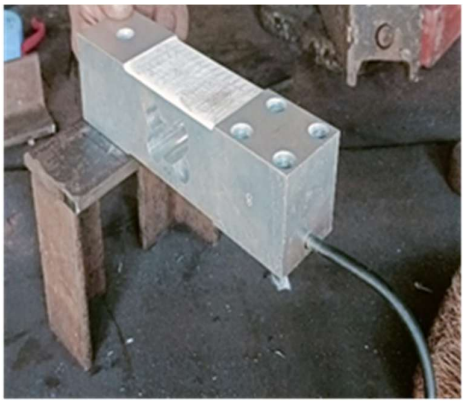

**Plate 3.10 Angle iron stools for mounting the load cells**

### 3.3.3 Sensor integration and electronic circuit assembly

For the electronic integration of the Smart Weighing Lysimeter, all sensors and modules were systematically interfaced with an ATmega-based Arduino microcontroller to enable continuous monitoring and precise data logging. Four individual load cells were each connected to separate HX711 load cell amplifiers, which served to amplify and convert the analog signals from the strain gauges into digital signals readable by the Arduino as shown in Plate 3.6. Each HX711 module had its VCC and GND pins connected to a common power rail on a breadboard, which was powered by the 5V and GND pins of the Arduino. The digital communication lines, DATA (DT) and CLOCK (SCK) pins of the HX711 modules were connected to specific

digital I/O pins on the Arduino: for example, load cell 1 was connected to pins 5 (DT) and 6 (SCK), load cell 2 to pins 7 and 8, load cell 3 to pins 9 and 10, and load cell 4 to pins 11 and 12, respectively as represented in Plate 3.7. This configuration allowed independent readings from each load cell to calculate the individual and total weight of the soil-plant system.

To monitor environmental conditions, a DHT22 sensor was connected to the Arduino to measure ambient temperature and relative humidity. The DHT22's data pin was connected to digital pin 24 on the Arduino, while its VCC and GND were linked to the 5V and GND rails on the breadboard. These environmental sensors provided critical context for interpreting plant-water-soil interactions in the lysimeter.

A 20x4 Liquid Crystal Display (LCD) with an I2C interface was included to visually display real-time data such as temperature, humidity, the total weight measured by the load cells. The LCD's SDA and SCL lines were connected to the Arduino's dedicated I2C pins-SDA to pin 20 and SCL to pin 21. Additionally, a DS3231 Real-Time Clock (RTC) module was incorporated to provide accurate time-stamping for the sensor data. This RTC module also used the I2C protocol and shared the same SDA and SCL lines (pins 20 and 21) with the LCD, as I2C allows multiple devices to operate on the same communication bus.

For data storage, a microSD card module was connected to the Arduino, enabling long-term data logging. The module's CS (chip select) pin was connected to digital pin 53, while MOSI, MISO, and SCK were connected to pins 51, 50, and 52 respectively, aligning with the SPI communication standard on the Arduino Mega. Power (VCC) and ground (GND) were also connected via the breadboard rails. The SD card was formatted and mounted appropriately to ensure reliable data writing and retrieval.

All components, including sensors, modules, and communication buses, were interconnected using male-to-male jumper wires on a standard breadboard. This comprehensive and neatly organized integration enabled the Smart Weighing Lysimeter to function as a fully automated system capable of capturing real-time environmental data and soil-plant dynamics with high accuracy and temporal resolution. The inclusion of time-stamped data logging ensured that the system could be reliably used for

applications such as evapotranspiration estimation, irrigation scheduling, and soil-water balance studies in agricultural research. Plate 3.11 shows Block diagram of Electronic Circuit and Plate 3.12 shows Electronic Circuit Assembly.

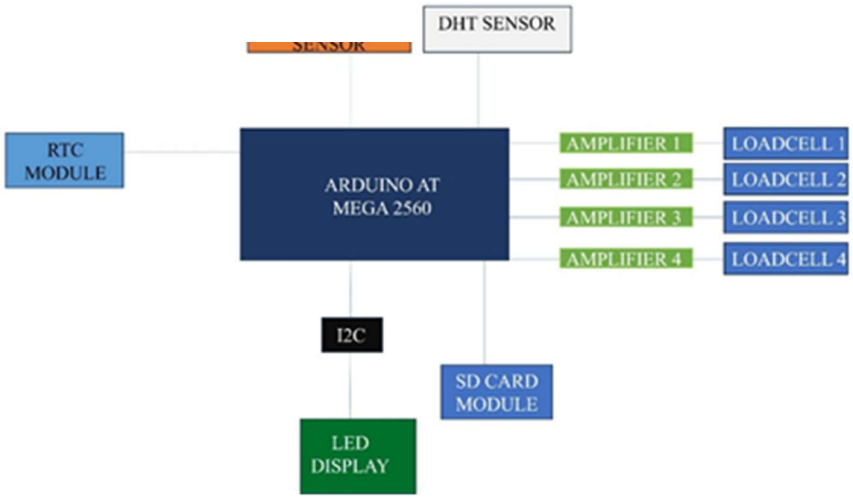


**Plate 3.11 Block diagram of electronic circuit**

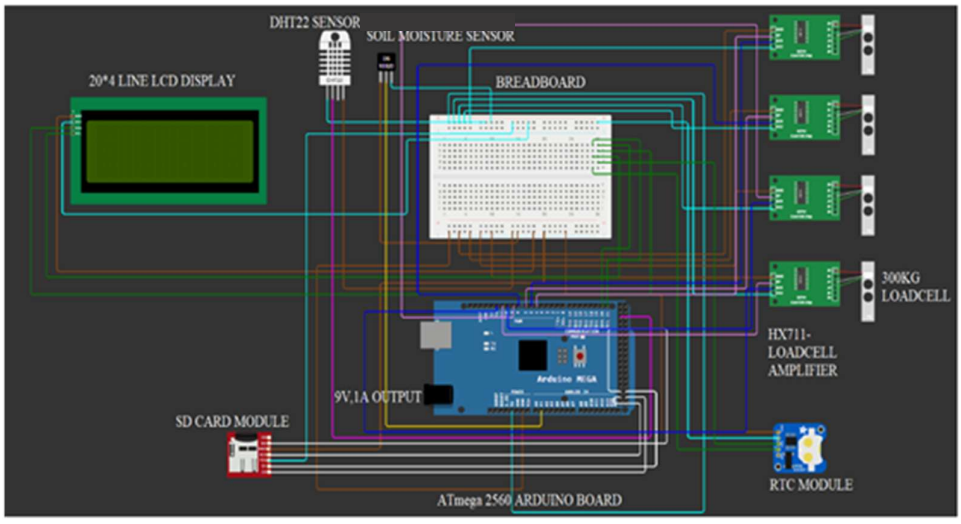


**Plate 3.12 Electronic circuit assembly**

The components used in the circuit assembly are:

### *3.3.3.1 HX711 Amplifier module*

The HX711 Amplifier module (Plate 3.13) is a precision 24-bit analog-to-digital converter (ADC) designed specifically for weigh scale and industrial control applications. It integrates a high-precision low-noise programmable gain amplifier (PGA) and supports two differential input channels. With a selectable gain of 32, 64, or 128 and on-chip power regulation, the HX711 allows easy and accurate interfacing of load cells with any microcontroller. It requires no external amplifier or dual power supply, making it a cost-effective and reliable solution for digital weighing systems. Table 3.1 shows the specification of HX711 Amplifier Module.

**Table 3.1 Specification of HX711 amplifier module**

| **Parameter** | **Specification** |
|---|---|
| Operating Voltage Range | 3 – 5 V |
| ADC Resolution | 24-bit |
| Differential Input Channels | 2 |
| Programmable Gain | 32, 64, 128 (on-chip PGA) |
| Output Data Rate | 10 SPS or 80 SPS (selectable) |
| On-chip Power Supply Regulator | For load cell and ADC analog power |
| On-chip Oscillator | Yes (optional external crystal supported) |
| Supply Rejection | Simultaneous 50 Hz and 60 Hz |
| Communication Interface | Two-wire (Clock and Data) |
| Control Interface | Simple digital pin-driven, no programming needed |
| Features | High precision, low noise, low cost, high reliability |
| Cost | ₹ 44/- |

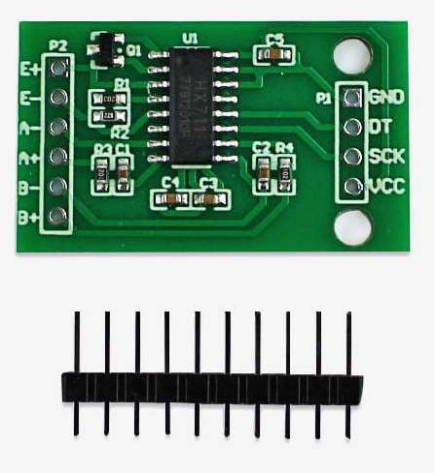


**Plate 3.13 HX711 amplifier**

### *3.3.3.2 Microcontroller board*

The Arduino ATmega 2560 (Plate 3.14) is a microcontroller board based on the ATmega2560, designed for complex projects requiring more I/O pins, memory, and processing power. It features 54 digital input/output pins (of which 15 can be used as PWM outputs), 16 analog inputs, 4 UARTs (hardware serial ports), a 16 MHz crystal oscillator, USB connection, power jack, ICSP header, and a reset button. The board can be powered via USB, battery, or an external adapter. With a large number of pins and increased memory, it is well-suited for applications involving multiple sensors, actuators, or communication modules. Table 3.2 shows the specification of Arduino Atmega 2560.

**Table 3.2 Specification of arduino Atmega 2560**

| Parameter | Specification |
|---|---|
| Microcontroller | ATmega2560 |
| Operating Voltage | 5 V |
| Recommended Input Voltage | 7 – 12 V |
| Input Voltage (limit) | 6 – 20 V |
| Digital I/O Pins | 54 (15 provide PWM output) |
| Analog Input Pins | 16 |

| Parameter | Specification |
|---|---|
| DC Current per I/O Pin | 40 mA |
| DC Current for 3.3V Pin | 50 mA |
| Flash Memory | 256 KB (8 KB used by bootloader) |
| SRAM | 8 KB |
| EEPROM | 4 KB |
| Clock Speed | 16 MHz |
| USB Host Chip | MAX3421E |
| Board Length | 101.52 mm |
| Board Width | 53.3 mm |
| Weight | 36 g |
| Cost | ₹1199 /- |


**Plate 3.14 Arduino ATmega 2560**

### *3.3.3.3 CZL 642 300 kg load cell*

The CZL 642 (Plate 3.15) is a high-precision single-point load cell made of aluminum alloy with anodized treatment, offering IP65 protection. It is widely used in electronic weighing scales, retail, bench, and counting scales. With a C3 class precision rating, it ensures excellent accuracy, stability, and durability under variable environmental conditions. It operates on 5–12 V DC excitation and provides a rated

output of 2.0 mV/V ±5%. The CZL 642 is capable of measuring loads up to 300 kg, with high resistance to overloads (up to 200% of full scale), making it reliable for long-term weighing applications. Table 3.3 shows the specification of CZL 642 300 kg load cell.

**Table 3.3 Specification of CZL 642 300 kg load cell**

| Parameter | Specification |
|---|---|
| Type | Single Point Load Cell |
| Material | Aluminum Alloy |
| Surface Treatment | Anodized |
| Protection Class | IP65 |
| Rated Load | 300 kg |
| Rated Output | 2.0 mV/V ± 5% |
| Zero Balance | ±1% Full Scale |
| Input Resistance | 405 ± 6 Ohm |
| Output Resistance | 350 ± 3 Ohm |
| Excitation Voltage | 5 – 12 V DC |
| Total Precision Class | C3 Class |
| Nonlinearity | 0.017% Full Scale |
| Hysteresis | 0.02% Full Scale |
| Repeatability | 0.01% Full Scale |
| Creep (30 minutes) | 0.015% Full Scale |
| Operating Temperature Range | -20°C to +65°C |
| Temperature Effect on Zero | 0.017% Full Scale / 10°C |
| Temperature Effect on Span | 0.014% Full Scale / 10°C |
| Insulation Resistance | ≥5000 MΩ (50 V DC) |
| Safe Overload Capacity | 150% Full Scale |
| Ultimate Overload Capacity | 200% Full Scale |

| Parameter | Specification |
|---|---|
| Cable | 420 mm (3 mm dia, 4-wire shielded cable) |
| Cost | ₹637.20 |


**Plate 3.15 CZL 642 300 kg load cell**

### *3.3.3.4 DHT22 (AM2302) temperature and humidity sensor*

The DHT22 (AM2302) (Plate 3.16) is a high-accuracy digital sensor designed for simultaneous measurement of temperature and humidity. It integrates a capacitive humidity sensor and a thermistor, providing calibrated digital output suitable for microcontrollers such as Arduino, Raspberry Pi, and ESP boards. With a measurement range of -40°C to +80°C for temperature and 0–100% RH for humidity, it is well-suited for applications like weather monitoring, greenhouses, HVAC systems, and data logging. The sensor offers high-resolution readings (0.1°C and 0.1% RH) with long-term stability, featuring annual deviations within ±1°C for temperature and ±1% RH for humidity. Its digital output simplifies circuit design by eliminating the need for analog-to-digital conversion. Operating at 3 to 5.5V and consuming low current, the DHT22 communicates via a single-wire interface and comes in a compact 4-pin plastic enclosure (using only VCC, GND, and DATA), making it easy to integrate into various

setups. Table 3.4 shows Specification of DHT22 (AM2302) Temperature and Humidity Sensor. Plate 3.16 shows DHT22 (AM2302) Temperature and Humidity Sensor.

**Table 3.4 Specification of DHT22 (AM2302) temperature and humidity sensor**

| **Parameter** | **Specification** |
|---|---|
| Sensor Type | Temperature and Humidity Sensor |
| Model Number | AM2302 |
| Operating Voltage | 3.0 to 5.5 V |
| Temperature Measurement Range | -40°C to +80°C |
| Humidity Measurement Range | 0% to 100% RH |
| Temperature Accuracy | ±0.5°C |
| Humidity Accuracy | ±2% RH (in 10–90% RH range) |
| Temperature Resolution | 0.1°C |
| Humidity Resolution | 0.1% RH |
| Output Type | Digital (Calibrated Signal) |
| Communication Protocol | Single-wire serial interface |
| Long-Term Stability | Temp: <1°C/year, Humidity: <1% RH/year |
| Temperature Compensation | Full-range built-in |
| Contact Type | 4-pin (VCC, GND, DATA; 1 unused) |
| Reusability | High |
| Dimensions (L × W × H) | Approx. 43 mm × 15 mm × 10.7 mm |
| Weight | 15 g |
| Adhesive Backing | No |
| Mounting Options | Custom casing or enclosure recommended |
| Shipping Weight | 0.01 kg |
| Shipping Dimensions | 5 × 4 × 2 cm |
| Typical Applications | Weather stations, greenhouses, HVAC systems, data loggers, indoor air. |

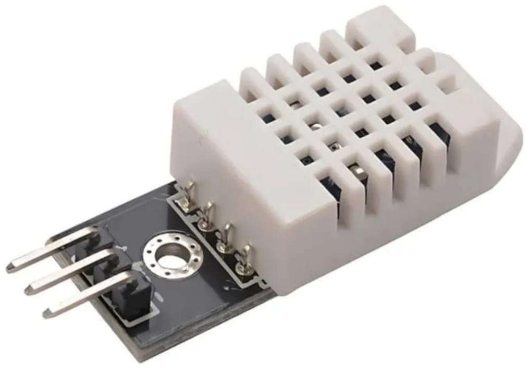

**Plate 3.16 DHT22 (AM2302) temperature and humidity sensor**

### *3.3.3.5 SD card module*

The SD Card Module (Plate 3.17) is a compact and reliable interface board that allows microcontrollers such as Arduino, ESP32, and Raspberry Pi to read from and write to SD cards. It is commonly used for data logging, audio, video, and other file storage applications. The module operates on 4.5V–5.5V input and features an onboard 3.3V voltage regulator, making it compatible with both 5V and 3.3V logic levels. It uses SPI communication (MISO, MOSI, SCK, CS) and is equipped with M2 mounting holes for secure installation. Its compact size and lightweight design make it ideal for embedded applications. Table 3.5 shows specification of SD Card Module.

**Table 3.5 Specification of sd card module**

| **Parameter** | **Specification** |
|---|---|
| Power Supply Voltage (VDC) | 4.5 to 5.5 |
| Voltage Regulator | 3.3V |
| Control Interface | GND, VCC, MISO, MOSI, SCK, CS |
| Mounting Hole Size | M2 (4 holes, 2.2 mm diameter) |
| PCB Size (L × W) mm | 40 × 24 mm (also noted as 45 × 28 mm) |
| Weight (g) | 6 |
| Shipping Weight | 0.005 kg |
| Shipping Dimensions | 9 × 5 × 2 cm |
| Price | ₹ 38 |


**Plate 3.17 SD Card Module**

### *3.3.3.6 20×4-line lcd display*

The 20×4 Line LCD Display from Silicon TechnoLabs (Plate 3.18) is a versatile alphanumeric display module designed for a wide range of embedded applications. With a blue backlight and the ability to display 4 lines with 20 characters per line, it provides a clear, high-contrast viewing experience. It features a built-in HD44780-equivalent controller, making it compatible with popular microcontrollers such as Arduino, Raspberry Pi, AVR, ARM, and 8051. Operating at 5V DC, this LCD is ideal for student projects, educational setups, and industrial applications including copiers, routers, fax machines, and test equipment. Table 3.6 shows specification of 20×4 Line LCD Display.

**Table 3.6 Specification of 20×4 line lcd display**

| **Parameter** | **Specification** |
|---|---|
| Brand | Silicon TechnoLabs |
| Manufacturer | Silicon TechnoLabs |
| Country of Origin | India |
| Model Number | ST/20x4B |
| Display Type | Character LCD with Blue Backlight |
| Display Size | 20 characters × 4 lines |
| Controller | HD44780 Equivalent |
| Voltage | 5V DC |
| Compatible Devices | Arduino, Raspberry Pi, AVR, ARM, 8051 |
| Special Features | Wide viewing angle, high contrast, LCM character type |
| Intended Use | Student Projects, Industrial Devices, Educational Kits |
| Weight | 90 g |

| | |
|---|---|
| Package Dimensions | 11.2 × 8.6 × 2.8 cm |
| Power Source | DC |
| Processor Brand (Unrelated) | ARM (Note: Not applicable directly to the LCD but might refer to MCU use) |
| Operating System (Incorrect) | blogspot (Disregard – LCD doesn't use OS) |
| Maximum Memory Supported | 1 GB (Not applicable to display) |
| Batteries Included | No |

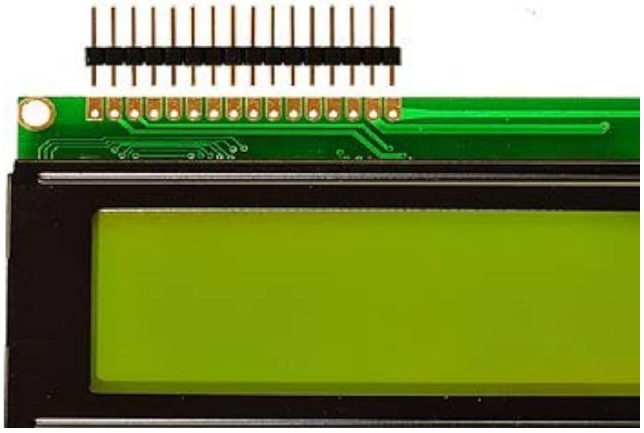

**Plate 3.18 20×4-line lcd display**

***3.3.3.7 Jumper wires – male to male, male to female, female to female***

These jumper wires (Plate 3.19) are made with high-quality materials and advanced techniques, ensuring reliable performance in electronic projects. Each wire is approximately 20 cm (8-inch) long, offering ample length for connecting various components on a breadboard or development board. The male connectors are designed to fit into standard 0.1 inch (2.54 mm) female sockets, while the female connectors are compatible with standard 0.1 inch male headers. They are ideal for temporary circuit connections, prototyping, and interfacing microcontrollers with sensors and modules. These wires are durable, reusable, and well-suited for educational and DIY electronics projects. Table 3.7 shows specification of Jumper Wires**.**

**Table 3.7 Specification of jumper wires**

| Parameter | Specification |
|---|---|
| Wire Types | M2M (Male-to-Male), M2F (Male-to-Female), F2F (Female-to-Female) |
| Cable Length | 20 cm (8 inches) |
| Connector Pitch | 2.54 mm (0.1 inch) |
| Material Quality | Premium |
| Reusability | High (Solderless and Durable) |
| Applications | Breadboarding, Prototyping, Microcontroller Connections |

**Plate 3.19 Jumper wires**

### *3.3.3.8 Sandisk micro sd/sdhc 16gb class 10 memory card*

The SanDisk Micro SD/SDHC 16GB Class 10 Memory Card (Plate 3.20) is a high-speed, reliable storage solution ideal for mobile devices, Raspberry Pi, and other embedded systems. With a data transfer rate of up to 98MB/s, it ensures fast and efficient performance for applications requiring quick data access and storage. The Class 10 rating guarantees consistent minimum write speeds, making it suitable for HD video recording and high-resolution image capture. Backed by a 5-year manufacturing defect warranty from SanDisk, this memory card offers both durability and dependable performance for a wide range of electronics and embedded systems projects. Table 3.8 shows specification of SanDisk Micro SD/SDHC 16GB Memory Card.

**Table 3.8 Specification of sandisk micro sd/sdhc 16gb memory card**

| Parameter | Specification |
|---|---|
| SKU | 303315 |
| Memory | 16 GB |
| Item Type | Memory Card |

| | |
|---|---|
| Model | SanDisk Micro |
| Model Type | Micro SD/SDHC |
| Series | Series |
| Class Type | Class 10 |
| Data Transfer Rate | Up to 98 MB/s |
| Card Type | Micro SD |
| Warranty | 5 Years (Manufacturing Defects by SanDisk) |
| Applications | Mobile Phones, Raspberry Pi, Embedded Projects |
| UPC | 6.19659E+11 |
| Shipping Weight | 0.06 kg |
| Shipping Dimensions | 10 × 7 × 3 cm |


**Plate 3.20 SanDisk micro sd/sdhc 16gb memory card**

### *3.3.3.9 Breadboard*

The 400 Tie Points Mini Circuit Experiment Solderless Breadboard (Plate 3.21) is a compact prototyping tool ideal for building and testing electronic circuits without soldering. It features 400 contact points divided into power rails and terminal strips, allowing easy component placement and jumper wire connections. The board uses a spring clip design that securely holds wires and components, making it reusable and suitable for educational and experimental setups. This breadboard is compatible with various components like resistors, capacitors, ICs, and microcontrollers. It supports 20–29 AWG jumper wires and can be interconnected with other breadboards for larger projects. Its adhesive backing and interlocking sections make it versatile and convenient to mount on different surfaces. Table 3.9 shows specification of Breadboard.

**Table 3.9 Specification of breadboard**

| Parameter | Specification |
|---|---|
| Total Tie Points | 400 |
| Terminal Strips | 1 (300 Tie Points) |
| Power Rails | 2 (100 Tie Points) |
| Contact Type | Spring Clip (Nickel-plated) |
| Wire Compatibility | 20–29 AWG |
| Reusability | High (Solderless) |
| Dimensions | Approx. 8.2 cm × 5.4 cm × 0.85 cm |
| Adhesive Backing | Yes |
| Interlocking Sections | Yes |
| Typical Applications | Prototyping, Circuit Testing, Education |

**Plate 3.21 Breadboard**

***3.3.3.10 DS3231 RTC memory module***

The DS3231 RTC Memory Module (Plate 3.22) is a highly accurate real-time clock that uses an integrated temperature-compensated crystal oscillator (TCXO) to maintain precise timekeeping. It operates via an I2C interface and is capable of tracking seconds, minutes, hours, day, date, month, and year with automatic leap year correction. The module includes a built-in lithium coin cell battery (CR2032) for maintaining time even during power outages, and some versions also feature a 32kbit EEPROM memory (AT24C32) for storing additional user data. Designed for low power consumption, the DS3231 offers excellent stability over a wide temperature range, making it ideal for

embedded systems and time-sensitive applications. Table 3.10 shows specification of DS3231 RTC Memory Module.

**Table 3.10 Specification of DS3231 RTC memory module**

| Parameter | Specification |
|---|---|
| RTC Chip | DS3231SN |
| Interface | I2C (Address: 0x68) |
| Voltage Range | 2.3V to 5.5V (typically 5V for Arduino) |
| Timekeeping Functions | Seconds, Minutes, Hours, Day, Date, Month, Year |
| Accuracy | ±2 ppm (0°C to +40°C), ±3.5 ppm (–40°C to +85°C) |
| Battery Type | CR2032 Lithium Coin Cell |
| Battery Backup | Yes, retains time during power loss |
| EEPROM (optional) | AT24C32 - 32kbit (4KB) non-volatile memory |
| Temperature Sensor | Built-in, ±3°C accuracy, 0.25°C resolution |
| SQW/32K Output | Optional square wave and 32kHz outputs |
| Power Consumption | ~2µA in battery mode |

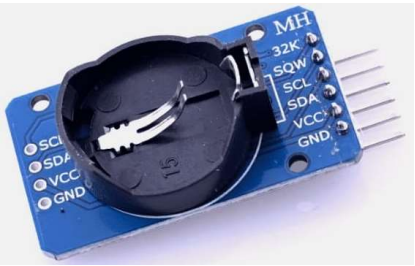


**Plate 3.22 DS3231 RTC memory module**

### *3.3.3.11 I2C (inter-integrated circuit) module*

The I2C (Inter-Integrated Circuit) module for a 20×4 LCD display (Plate 3.23) is a compact interface board that simplifies the wiring and control of character LCDs with microcontrollers like Arduino. It uses the I2C communication protocol, reducing

the number of required data lines from 6–8 to just two: SDA (data) and SCL (clock). The module is typically based on the PCF8574 I/O expander chip and comes with an onboard potentiometer for contrast adjustment and a jumper for backlight control. By soldering the module to the back of the LCD, users can quickly connect it to microcontrollers using only four wires (VCC, GND, SDA, and SCL), thus saving GPIO pins and enabling more compact and efficient circuit design. The I2C address can often be modified via jumpers on the module to prevent conflicts when using multiple devices on the same I2C bus. Table 3.11 shows Specification of I2C (Inter-Integrated Circuit).

**Table 3.11 Specification of I2C (inter-integrated circuit)**

| Parameter | Specification |
|---|---|
| Communication Protocol | I2C (Inter-Integrated Circuit) |
| Chipset | PCF8574 (I/O Expander) |
| Operating Voltage | 5V DC |
| Interface Pins | VCC, GND, SDA, SCL |
| Compatible Display | Standard 16×2 and 20×4 Character LCDs |
| I2C Address Range | 0x20 to 0x27 (can be configured via jumpers) |
| Potentiometer | Onboard for LCD contrast adjustment |
| Backlight Control | Jumper or software-controlled |
| Dimensions | Approx. 42mm × 19mm × 10mm |
| Mounting Type | Soldered directly to the LCD module |

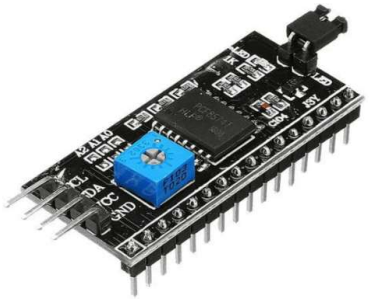


**Plate 3.23 I2C (inter-integrated circuit)**

### 3.3.4 System calibration

#### *3.3.4.1 Calibration of load cell*

Each CZL 300 kg load cell was calibrated individually to ensure accurate weight measurement in the smart lysimeter system. The Arduino Mega 2560 microcontroller was connected to a laptop via USB for programming and data monitoring. A suitable Arduino code was sourced and modified to match the load cell and HX711 amplifier configuration. The HX711 provided raw digital readings corresponding to the applied loads. Initially, the zero offset value (reading with no load) was recorded. Then, known weight of 6.1 kg was applied, and the raw readings were noted.

Using the relationship

$$\text{Weight (kg)} = \frac{\text{Raw Reading} - \text{Offset}}{\text{Calibration Factor}}$$

the calibration factor for each load cell was calculated by rearranging the formula:

$$\text{Calibration Factor} = \frac{\text{Raw Reading} - \text{Offset}}{\text{Weight (kg)}}$$

Based on this method, the calibration factors for the four load cells were determined and they are incorporated in the Arduino C++ code used for data acquisition. To ensure the reliability of the smart weighing lysimeter before use, the accuracy of the load cell system was verified by placing known standard weights on the lysimeter platform. The system was calibrated in the laboratory, and verification involved placing incremental weights (e.g., 5 kg, 10 kg, 15 kg, etc.) and comparing the recorded values with actual weights.

### 3.3.5 Sensor connection and data acquisition

Following the calibration, the hardware system was fully assembled. The Arduino Mega 2560 was interfaced with various sensors: a DHT22 sensor for temperature and relative humidity, four calibrated load cells connected via HX711 amplifiers through a summing circuit. The Arduino code was further modified to integrate all sensors and enable synchronized data acquisition. The entire system was powered using a 9V, 1A battery. Real-time data, including temperature, humidity, cumulative weight from the load cells, were collected at one-minute intervals. These

values were simultaneously displayed on an LCD screen and logged into a microSD card through the SD card module for continuous data storage and further analysis . Plate 3.24 shows Sensor Connection and Display.


**Plate 3.24 Sensor Connection and Display**

3.4 FIELD EXPERIMENTAL DETAILS

The experimental study was carried out within a naturally ventilated polyhouse over a period extending from April 9 to May 31, 2025. The total duration of the crop cycle was approximately 30-40 days. The polyhouse structure was aligned in (Plate 3.25) the east–west direction, with dimensions of 26 meters in length and 8 meters in width. This setup allowed for assessing crop performance and environmental conditions for protected cultivation systems. Table 3.12 shows description of Polyhouse.

**Table 3.12 Description of polyhouse**

| **Parameter** | **Value** |
|---|---|
| Area | 213 m² |
| Length | 26 m |
| Width | 8 m |
| Centre height | 6 m |
| Gutter height | 3.5 m |


**Plate 3.25 Polyhouse**

### 3.4.1 Field preparation

Land preparation was carried out within the naturally ventilated polyhouse to facilitate the experimental activities. A specific portion of the polyhouse area was allocated exclusively for establishing the experimental setup. In this allocated space, three raised beds were constructed, each having dimensions of 1.0m ×1.0m × 0.3m to cultivate *Amaranthus dubius.*

### 3.4.2 Preparation of growing media

The soil preparation was carried out meticulously to create optimal growing conditions for *Amaranthus dubius* in a 4 m² plot. The site was selected based on its sandy loam texture, which offers excellent drainage, root penetration, and ease of cultivation qualities particularly well-suited for leafy vegetables like *Amaranthus dubius*.

The plot was initially cleared of weeds and debris, and the topsoil was loosened to a fine tilth by thorough hand hoeing. This helped improve soil aeration and facilitated the uniform mixing of soil amendments. To enhance soil fertility and microbial activity, 2 kg of Trichoderma-enriched coir pith was incorporated evenly into the soil. This organic amendment not only serves as a bio-control agent against soil-borne pathogens but also improves the water-holding capacity and structure of the sandy loam. To further boost the nutrient content, 10 kg of well-powdered cow dung was added. Being rich in essential nutrients and beneficial microorganisms, cow dung plays a vital role in promoting plant growth and improving soil organic matter. Additionally, 200 g of finely

powdered limestone (calcium carbonate) was mixed into the topsoil to correct soil acidity, increase calcium availability, and enhance nutrient uptake efficiency by the crop (plate 3.26). All the inputs were thoroughly mixed into the top 15–20 cm of soil, and the bed was levelled to ensure even sowing and water distribution. The prepared soil provided a biologically active and nutrient-rich environment, supporting healthy germination and vigorous early growth of *Amaranthus dubius* plants. Plate 3.26 shows Soil preparation in the lysimeter tank

**Plate 3.26 Soil preparation in the lysimeter tank**

### 3.4.3 Experimental setup

A single smart Weighing lysim$_{et}$er unit was constructed and assembled in the research workshop. The fabricated lysimeter tank had dimensions of 110 cm × 80 cm ×60 cm and weighed 117.5 kilograms. Once the fabrication and sensor integration were completed, the entire setup was carefully transported to the naturally ventilated polyhouse for installation. A pit measuring 1.5m × 1.5m × 0.6m was excavated at the designated location within the polyhouse. The specially fabricated angle iron stand was positioned inside the pit to support the lysimeter structure. The entire lysimeter assembly, including the tank mounted on load cells and electronic components, was securely placed on this stand inside the pit to ensure stability and accurate measurement as represented in Plate 3.27

**Plate 3.27 Experimental setup of the smart weighing lysimeter**

### 3.4.4 Crop details

Coimbatore Co.1 (*Amaranthus dubius)* was selected as the experimental crop to estimate crop evapotranspiration in this study. This variety, developed at Tamil Nadu Agricultural University (TNAU) was specifically chosen for its tender leaves and mature stems. It is highly suited for late harvesting and is not recommended for the clipping method of leaf harvest. Under optimal conditions, it can yield approximately 7–8 tonnes per hectare within 30 days of growth.

Seedlings of *Amaranthus dubius* were initially raised at the Nursery of Krishi Vigyan Kendra (KVK), Malappuram. The nursery period lasted for approximately 30 days. Transplanting was carried out after this period, and the seedlings were carefully transplanted into the Lysimeter and and surrounding beds at the experimental site. Plate 3.28 shows the field view after transplanting of *Amaranthus dubius* in the lysimeter tank and Plate 3.29 shows the field view after 15 days of transplanting of *Amaranthus dubius* in the lysimeter tank.

**Plate 3.28 Field view after transplanting *Amaranthus dubius* in the lysimeter tank**

**Plate 3.29 Field view after 15 days of transplanting *Amaranthus dubius* in the lysimeter tank**

### 3.4.5 Irrigation system

A 50 mm diameter PVC sub-main line was connected to the main irrigation supply, and 12 mm diameter low-density polyethylene (LDPE) laterals were laid out from this sub-main to distribute water within the polyhouse. End caps were attached to the ends of all laterals to maintain adequate pressure and ensure uniform water delivery along the system.14 Emitters of 2 lph discharge were provided inside the tank. Irrigation was scheduled every day at 8:00 AM. Instead of using fixed crop coefficients or reference evapotranspiration values, irrigation was applied in slightly excess quantities to guarantee that the crop's water requirements were fully met. This ensured that evapotranspiration occurred at its potential rate, while also preventing any risk of moisture stress. The strategy was especially suited for the controlled polyhouse environment, where consistent soil moisture conditions are critical for accurate evapotranspiration studies.

## 3.5 WEIGHT DYNAMICS IN POLYHOUSE CULTIVATION

To evaluate the diurnal variation in evapotranspiration, hourly weight changes of the weighing lysimeter were recorded after planting of *Amaranthus dubius*. Data collection began at 08:00 a.m, the weight of the lysimeter was recorded hourly until 07:00 p.m. To determine the hourly evapotranspiration, the weight at each hour was

subtracted from the weight recorded during the previous hour. This hourly weight loss was attributed primarily to evapotranspiration, assuming negligible drainage or water input during the period. This procedure enabled the identification of peak evapotranspiration hours.

## 3.6 DETERMINATION OF $ET_C$

Field studies using weighing lysimeters are a precise method for estimating actual evapotranspiration ($ET_C$), as they provide direct measurements of water balance under field conditions (Abd and Ratshiedana, 2024). In this study, a weighing-type lysimeter fabricated using four load cells was employed to record real-time changes in the weight of the soil–plant system. This approach enables accurate quantification of evapotranspiration by capturing even minute changes in water input and output. The lysimeter was designed to isolate the soil column from the surrounding area to prevent seepage and to ensure vertical water flow (Zupanc *et al*., 2005).

### 3.6.1 Water balance data collection and calculation of $ET_C$

Crop evapotranspiration ($ET_C$) was determined using a smart weighing lysimeter system equipped with four individually calibrated load cells. These load cells continuously recorded the total weight of the lysimeter, which included soil, plant biomass, and water content. Irrigation was applied daily at 8:00 AM, and weight readings were taken before and after irrigation to assess the net change in water content. To measure water loss through drainage, a drainage outlet was installed at the base of the lysimeter, and a collection bottle was placed beneath it. Drainage water was collected and measured manually each day using a graduated measuring cylinder to ensure accurate estimation of water exiting the root zone. The lysimeter had a cross-sectional area of 110 cm × 80 cm (0.88 m²). Since 1 kg of water corresponds approximately to 1 litre, a conversion factor of 1.136 was used to convert the net change in weight (kg) into the depth of water applied or lost (mm/day) over the lysimeter area. The crop evapotranspiration ($ET_C$) was then calculated using the following equation:

$$ET_C\ (\text{mm/day}) = (\text{Weight after watering} - \text{Weight before watering} - \text{Drainage (L)}) \times 1.136$$

Where:

- Weight after watering = Lysimeter weight recorded after irrigation at 8:00 AM, (kg)
- Weight before watering = Lysimeter weight before irrigation on the next day (also around 8:00 AM), (kg)
- Drainage (L) = Volume of water drained from the lysimeter,
- 1.136 = Conversion factor (based on area 0.88 m²).

This approach allowed for direct measurement of $ET_C$ under real-time conditions, representing the actual water consumed by the crop through transpiration and evaporation.

## 3.7 COMPUTATION OF $ET_0$ USING CROPWAT

` CROPWAT is a decision support system developed by the Land and Water Development Division of the Food and Agriculture Organization (FAO) for the planning and management of irrigation. It is a computer-based program that estimates crop water requirements and irrigation scheduling by using climatic, crop, and soil data. The program utilizes the FAO Penman-Monteith method (FAO, 1992) to compute reference evapotranspiration ($ET_0$), which is a fundamental parameter in irrigation planning. In this study**,** minimum and maximum temperature data were obtained using a DHT22 sensor, which was installed alongside the load cell system in the experimental setup. The DHT22 sensor provided real-time measurements of ambient air temperature and relative humidity, from which the daily minimum and maximum temperatures were recorded. These temperature values were then manually input into the CROPWAT model to calculate daily $ET_0$ values. Plate 3.30 shows the view CROPWAT Model

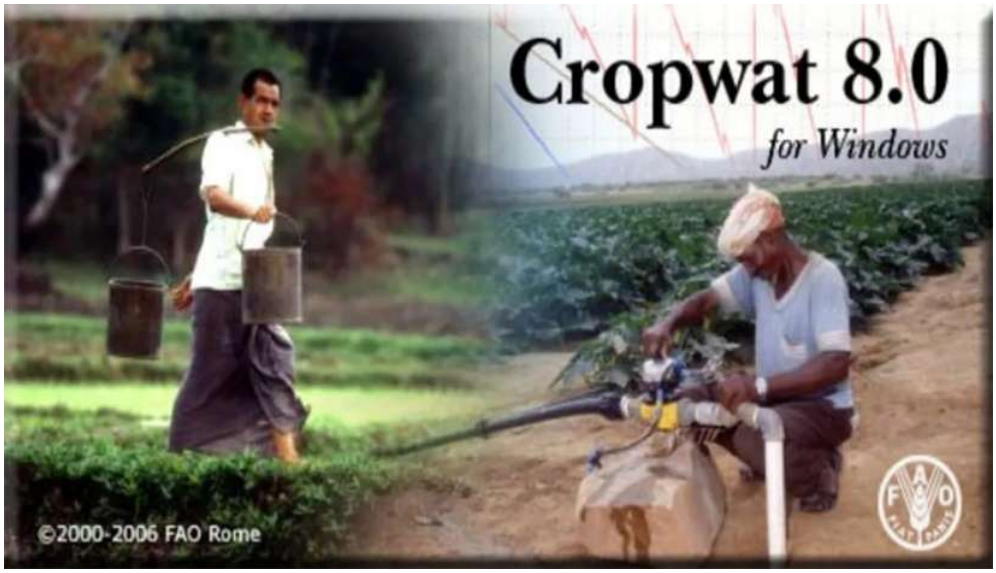


**Plate 3.30(a)**

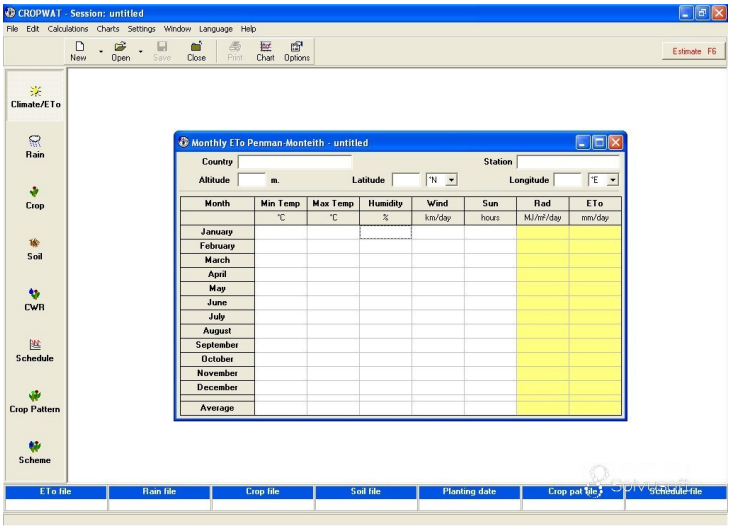


**Plate 3.30(b)**

**Plate 3.30 CROPWAT model**

### 3.7.1 Penman-monteith method

To calculate $ET_0$ using the Penman-Monteith method, Daily mean data are required, including maximum and minimum temperatures (°C).

The penman Monteith form of combination equation is,

$$ET_0 = \frac{0.408\Delta(R_n - G) + \gamma\frac{900}{T+273}U_2(e_s - e_a)}{\Delta + \gamma(1 + 0.34U_{2)}}$$

Where ,

$ET_0$: The reference evapotranspiration [mm/day]

$R_n$: The net radiation [MJ $m_{-2}$/day]

G: The soil heat flux density [MJ $m_{-2}$/day]

T: The mean daily air temperature at 2m height [$^oC$]

$U_2$: The wind speed at 2m height [km/day]

$E_s$: The saturation vapour pressure [KPa]

$E_a$: The actual vapour pressure [KPa]

($e_s$-$e_a$): The vapour pressure deficit of the air [KPa]

Δ: The slope vapour pressure curve [KPa $^oC^{-1}$]

γ: The psychometric constant [KPa $^oC^{-1}$]

### 3.7.2 Data requirements for CROPWAT

In this study climate data of polyhouse in Tavanur region was given as input to the CROPWAT. The climatic data include maximum and minimum temperatures (ºC), mean daily relative humidity (%), daily sunshine (hours) and wind speed (km/day).

#### *3.7.2.1 Climate data*

The daily data of minimum temperature and maximum temperature for one month were used to calculate radiation and $ET_o$. Minimum temperature, maximum temperature, and relative humidity were measured inside the polyhouse from April 2025 to May 2025 using the DHT22 sensor. Temperature and Humidity were measured at 6:30 am and 1.30 pm everyday based on IMD recommendations.

## 3.8 DEVELOPMENT OF CROP COEFFICIENT VALUES FOR *Amaranthus dubius*

ET rates of various crops are quantitatively related to the ET rate from a reference crop using crop coefficients (Allen *et al*., 1998). The crop coefficient ($K_c$) signifies the evapotranspiration ratio of a well-managed, disease-free crop grown under optimal water availability and soil fertility conditions to the evapotranspiration of a reference grass surface under the same environmental regime. Multiple factors influence the $K_c$ value, including crop type, phenological stage (growth phase),

microclimatic variables, and soil moisture status. $K_c$ is typically expressed as a time-dependent function throughout the crop's life cycle.

To determine the $K_c$ for *Amaranthus dubius*, cultivated exclusively under polyhouse conditions, the following methodology was undertaken:

Identification of the total duration of the crop cycle. Segmentation of the growing period into three principal stages: initial, mid-season, and late-season. Weekly estimation of ET for the *Amaranthus dubius* crop and reference ET ($ET_0$) using weighing lysimeters under the soil water balance method. The crop coefficient values for each growth stage were computed on a weekly basis using the relationship:

$$Kc = \frac{ET_C}{ET_0}$$

Where:

$ET_c$ crop is the actual evapotranspiration measured for *Amaranthus dubius*

$ET_0$ is the reference evapotranspiration.

Finally, crop coefficient curves were plotted to illustrate the temporal variation of $K_C$ values throughout the crop duration under polyhouse conditions.

## 3.9 CROP GROWTH AND YIELD PARAMETERS

To monitor the vegetative and reproductive performance of *Amaranthus dubius*, a set of growth and yield parameters were systematically observed. Three representative plants were randomly selected from within the lysimeter plot and were tagged immediately after transplanting for the purpose of consistent observation throughout the growing period. The following parameters were recorded:

### 3.9.1 Plant height

Plant height was measured from the base of the shoot to the tip of the apical meristem using a calibrated meter scale. Observations were taken daily, starting from the date of transplanting until the final harvest. This parameter served as a primary indicator of vegetative growth and was expressed in centimetres (cm). Variations in plant height were analysed to understand the influence of microclimatic conditions

under the polyhouse. Plate 3.31 shows the process of measuring plant height in the lysimeter setup.

**Plate 3.31 Measuring plant height**

### 3.9.2 Number of leaves

The number of fully expanded leaves per plant were counted manually each day in the tagged plants. This parameter provided insight into the canopy development of *Amaranthus dubius*, which is directly related to photosynthetic efficiency and potential biomass accumulation. These counts were recorded and later plotted for trend analysis.

### 3.9.3 Yield parameters

Harvesting of *Amaranthus dubius* commenced 40 days after sowing (DAS), as the crop had reached the tender leafy stage preferred for market consumption. During the harvest, the above-ground biomass was cut, leaving behind approximately 15 cm of the stem intact above the soil surface. This residual stem portion was preserved undisturbed, to promote rapid regeneration and maintain plant vigour for successive harvests. The biomass above the 15 cm mark was carefully removed using a sharp knife. The harvested biomass from each plant was weighed immediately using a digital

balance, and fresh weight was recorded accurately for the harvest. This yield data was used to evaluate the crop water productivity under controlled polyhouse conditions. Plate 3.32 shows the manual harvesting of *Amaranthus dubius* from the lysimeter setup.

**Plate 3.32 Harvesting of *Amaranthus dubius***

# *Results and discussion*

# CHAPTER IV
# RESULTS AND DISCUSSION

This chapter presents and discusses the findings of the study based on the objectives outlined. The design and development of the smart weighing lysimeter is first described in terms of its performance and functionality. The second section details the determination of crop evapotranspiration ($ET_C$) of *Amaranthus dubius* cultivated under a polyhouse environment, using data recorded from the developed lysimeter. Finally, the crop coefficient (Kc) of *Amaranthus dubius* is estimated by relating the observed $ET_C$ to reference evapotranspiration ($ET_0$). The results are analysed to assess the accuracy and applicability of the system for crop water requirement studies under protected cultivation.

## 4.1 CALIBRATION OF LOADCELLS

The smart weighing lysimeter system was developed using four individual load cells placed beneath the soil tank to capture weight changes associated with crop evapotranspiration. Each load cell was calibrated independently using a linear calibration formula, and the derived calibration factors were found to be -14.5, -14.25, -13.5, and -14.5 for Load Cells 1 through 4, respectively. These calibration values indicate a slight variation in sensitivity among the sensors, particularly for Load Cell 3, which exhibited a marginally lower response. Despite these variations, the overall system maintained acceptable consistency in load measurement when the readings were aggregated. The table 4.1 gives the calibration constants for loadcell 1 to 4 obtained using linear calibration formula.

To validate the accuracy of the lysimeter system post-calibration, a set of standard weights, ranging from 5 kg to 20 kg, were placed on the soil tank platform. The corresponding digital weight readings were recorded and compared against the actual weights. The results demonstrated that the lysimeter provided near-accurate weight estimations across all tested intervals. Although minor deviations were observed, they remained within an acceptable margin of error, confirming the practical reliability of the system. The deviation was primarily attributed to load distribution asymmetry, minor mechanical flexing, and slight sensor non-linearities, particularly noticeable at higher weight values. Similar trend in calibration of load cell curve was

obtained by Sagar *et al*., 2015, in his study on Development of Smart weighing lysimeter for measuring evapotranspiration and developing crop coefficient for greenhouse chrysanthemum. The table 4.2 gives observed weight when a standard weight was placed on the loadcells. Graphical representation of the relationship between observed and standard weight is given in figure 4.1.

**Table.4.1 Calibration constants for each load cell**

| Load Cell Number | Calibration Value |
|---|---|
| 1 | -14.5 |
| 2 | -14.25 |
| 3 | -13.5 |
| 4 | -14.5 |

**Table.4.2 Comparison of standard weights and observed weights during load cell calibration**

| Standard Weight (kg) | Observed Weight (kg) |
|---|---|
| 5 | 5.02 |
| 7.5 | 7.51 |
| 10 | 10.02 |
| 12.5 | 12.51 |
| 15 | 15.02 |
| 17.5 | 17.51 |
| 20 | 20 |

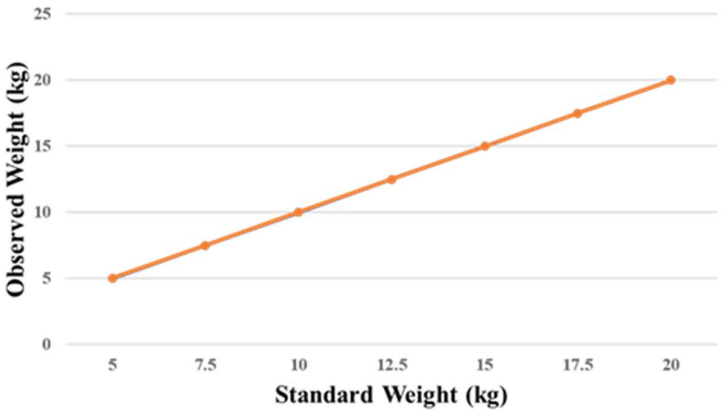


**Fig.4 .1 Relationship between standard and observed weights during calibration**

## 4.2 PHYSICAL PROPERTIES OF SOIL

### 4.2.1 Bulk density and dry density

Bulk density and dry density of the soil filled in the Lysimeters were measured using core cutter method. The value of bulk density and dry density were observed as 1.7 g/cc and 1.58 g/cc, respectively. Similar values were obtained from Madhavi (2017) in her study on the comparative evaluation of evapotranspiration parameters in a naturally ventilated polyhouse and an open field.

## 4.3 WEIGHT DYNAMICS IN POLYHOUSE CULTIVATION

The irrigation dynamics within the plant–soil–water system were assessed by monitoring weight variations recorded by the developed smart lysimeter. The water balance data provided accurate tracking of water loss throughout the entire cropping period. After each irrigation event, the weight of the cultivation tank initially increased, followed by a gradual decrease as the crop absorbed water, which is consistent with expected behaviour. At the onset of drainage through the soil profile, a rapid drop in tank weight was observed. This was later followed by a slower decline attributed to the crop's water uptake. Since the crop was grown under greenhouse conditions, no rainfall occurred, and thus no external water input influenced the soil moisture beyond field capacity. The weight data also captured minor fluctuations in the cultivation tank. Notably, a decrease in weight occurred during the daytime as a result of evapotranspiration.

In the lysimetric evaluation of *Amaranthus* cultivated within polyhouse setting, the hourly weight change was measured from 08:00 AM to 07:00 PM to estimate the rate of evapotranspiration across various growth stages. During the initial stage, the peak hourly weight change was observed to be approximately 0.41 kg, occurring between 01:00 PM and 02:00 PM. This value increased during the mid-stage, reaching a peak of around 0.68 kg within the same time interval. In the late stage, recorded just prior to harvest, the peak hourly change further increased to approximately 0.79 kg, again between 01:00 PM and 02:00 PM.The hourly data exhibited a distinct diurnal pattern, with a gradual increase in weight change from 08:00 AM, peaking during early afternoon, and subsequently showing a decline after 02:00 PM. This pattern reflects the

influence of environmental factors such as temperature, solar radiation, and humidity, which typically peak around midday. Similar trend in hourly change of load cell curve was obtained by Sagar *et al*., 2015, in his study on Development of Smart weighing lysimeter for measuring evapotranspiration and developing crop coefficient for greenhouse chrysanthemum. Figure 4.2 illustrates the hourly weight changes at different growth stages of *Amaranthus dubius* inside the polyhouse.

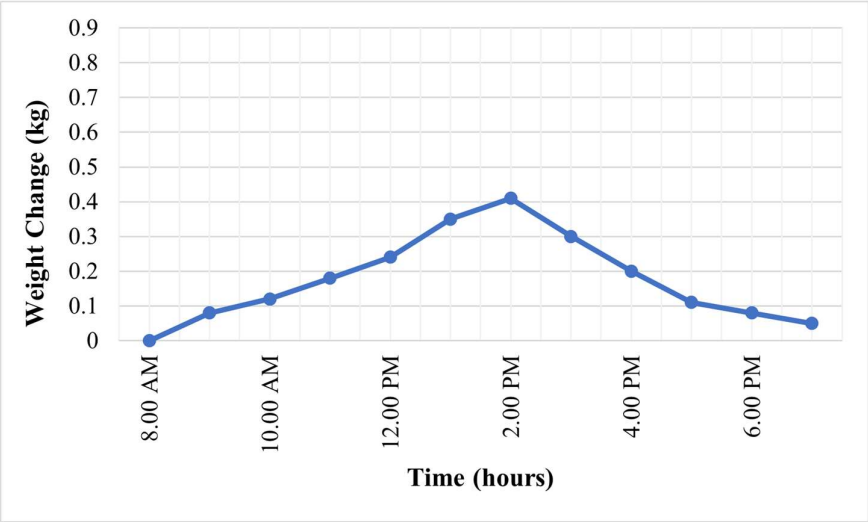


**Fig.4.2 a) Hourly weight change on 15-04-2025 (Initial stage)**

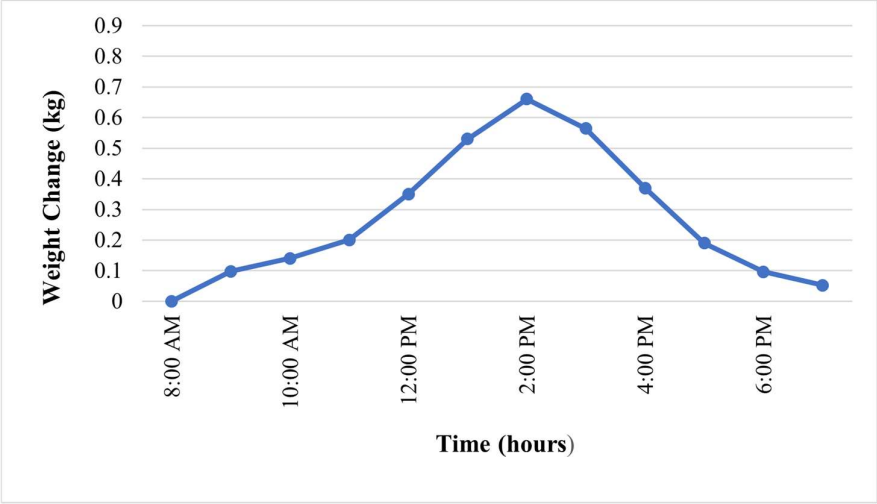


**Fig.4.2 b) Hourly weight change on 22-04-2025 (Mid stage)**

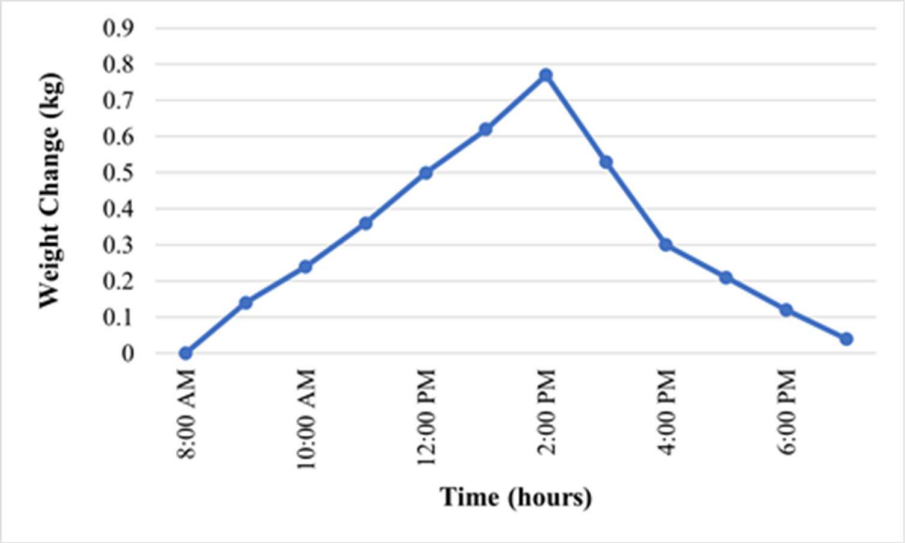


**Fig.4.2 c) Hourly weight change on 28-04-2025 (Late Stage)**

**Fig.4.2 Hourly weight change during different stages**

## 4.4 MICROCLIMATIC CONDITIONS INSIDE THE POLYHOUSE

During the crop growth period, the microclimatic conditions inside the polyhouse were continuously monitored. Temperature and relative humidity were recorded using the DHT22 sensors installed as part of the smart lysimeter system. Figure 4.5 presents the weekly average values of air temperature observed throughout the crop season inside the polyhouse. The maximum temperature of 41.3 °C and minimum temperature of 27.4 °C were noted during the crop growth period, the average temperatures ranged between 32.15°C to 34.65°C. These relatively stable temperatures inside the polyhouse created a favourable environment for plant growth. The controlled microclimate, especially the higher temperature compared to typical open field conditions, may contribute to early crop maturity and enhanced yield (Madhavi, 2017). The table 4.3 gives tabulated values of daily minimum, maximum and average temperature. Figure 4.3 gives the graphical representation of **variation of average temperature inside poly house during crop growth period.**

**Table.4.3 Temperature range and average temperature during crop period**

| S.no | Day | Min Temp | Max Temp | Avg Temp |
|---|---|---|---|---|
| 1 | 10-04-2025 | 28.5 | 38.5 | 33.5 |
| 2 | 11-04-2025 | 27.6 | 38.3 | 32.95 |
| 3 | 12-04-2025 | 27.9 | 38.3 | 33.1 |
| 4 | 13-04-2025 | 28 | 38.3 | 33.15 |
| 5 | 14-04-2025 | 28.1 | 36.3 | 32.2 |
| 6 | 15-04-2025 | 28.3 | 37.6 | 32.95 |
| 7 | 16-04-2025 | 28.4 | 36.3 | 32.35 |
| 8 | 17-04-2025 | 28.6 | 38.3 | 33.45 |
| 9 | 18-04-2025 | 28.3 | 38.4 | 33.35 |
| 10 | 19-04-2025 | 28.2 | 38.3 | 33.25 |
| 11 | 20-04-2025 | 27.5 | 41.3 | 34.4 |
| 12 | 21-04-2025 | 27.6 | 40.2 | 33.9 |
| 13 | 22-04-2025 | 28.2 | 40.9 | 34.55 |
| 14 | 23-04-2025 | 28.4 | 40.9 | 34.65 |
| 15 | 24-04-2025 | 27.8 | 38.5 | 33.15 |
| 16 | 25-04-2025 | 26.6 | 40.1 | 33.35 |
| 17 | 26-04-2025 | 26 | 40.1 | 33.05 |
| 18 | 27-04-2025 | 26 | 38.3 | 32.15 |
| 19 | 28-04-2025 | 29 | 39.8 | 34.4 |
| 20 | 29-04-2025 | 27.4 | 39.6 | 33.5 |
| 21 | 30-04-2025 | 26 | 39.5 | 32.75 |
| 22 | 1-05-2025 | 28 | 39.6 | 33.8 |

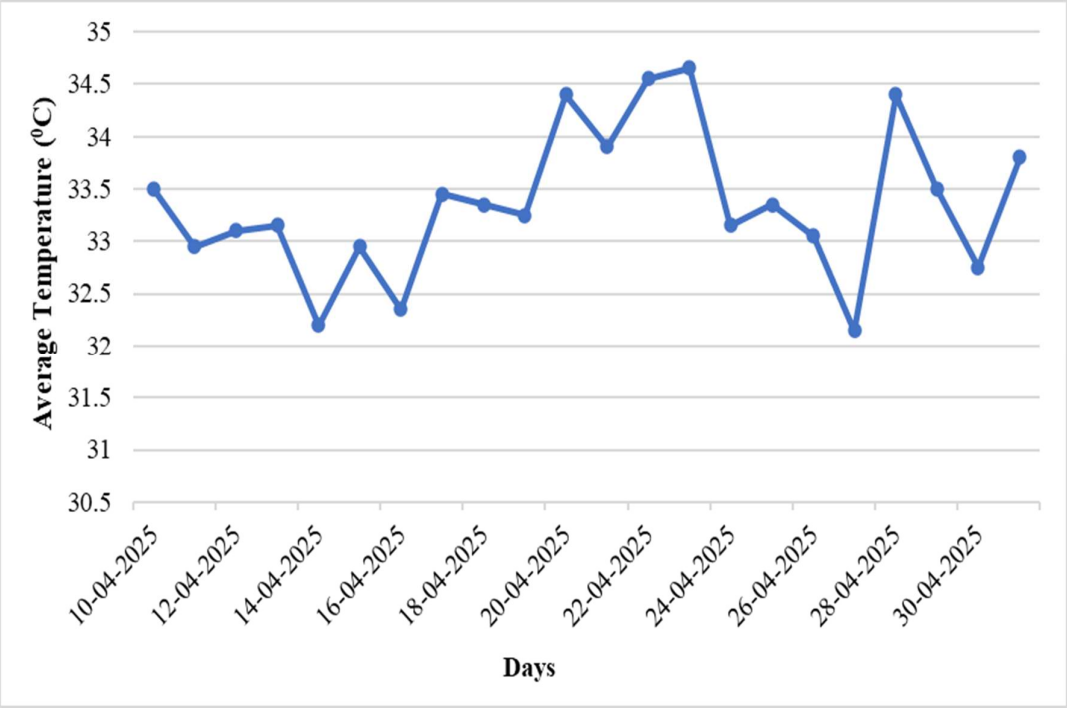


**Fig.4.3 Variation of average temperature inside poly house during crop growth period**

During the cropping period, the average relative humidity within the polyhouse environment was observed to range between 74% and 84%. This relatively high humidity regime created a favourable microclimatic condition for the cultivation of *Amaranthus dubius*, a crop that thrives under moderately humid conditions. The consistent atmospheric moisture levels likely contributed to enhanced transpiration regulation, better nutrient uptake, and vigorous vegetative growth throughout the growth stages. Moreover, the enclosed polyhouse setup played a crucial role in minimising external climatic fluctuations, thereby sustaining a relatively stable and conducive humidity environment for optimal physiological activity and biomass accumulation. The table 4.4 gives the tabulated value of average relative humidity inside polyhouse during crop growth period and the figure **4.4 gives the graphical representation of average relative humidity inside poly house during crop growth period.**

**Table.4.4 Variation of average relative humidity inside poly house during crop growth period**

| S.no | Day | Average Humidity(%) |
|---|---|---|
| 1 | 10-04-2025 | 79 |
| 2 | 11-04-2025 | 81 |
| 3 | 12-04-2025 | 80 |
| 4 | 13-04-2025 | 80 |
| 5 | 14-04-2025 | 81 |
| 6 | 15-04-2025 | 82 |
| 7 | 16-04-2025 | 84 |
| 8 | 17-04-2025 | 81 |
| 9 | 18-04-2025 | 79 |
| 10 | 19-04-2025 | 81 |
| 11 | 20-04-2025 | 74 |
| 12 | 21-04-2025 | 76 |
| 13 | 22-04-2025 | 77 |
| 14 | 23-04-2025 | 75 |
| 15 | 24-04-2025 | 79 |
| 16 | 25-04-2025 | 77 |
| 17 | 26-04-2025 | 74 |
| 18 | 27-04-2025 | 74 |
| 19 | 28-04-2025 | 79 |
| 20 | 29-04-2025 | 76 |
| 21 | 30-04-2025 | 74 |
| 22 | 1-05-2025 | 77 |

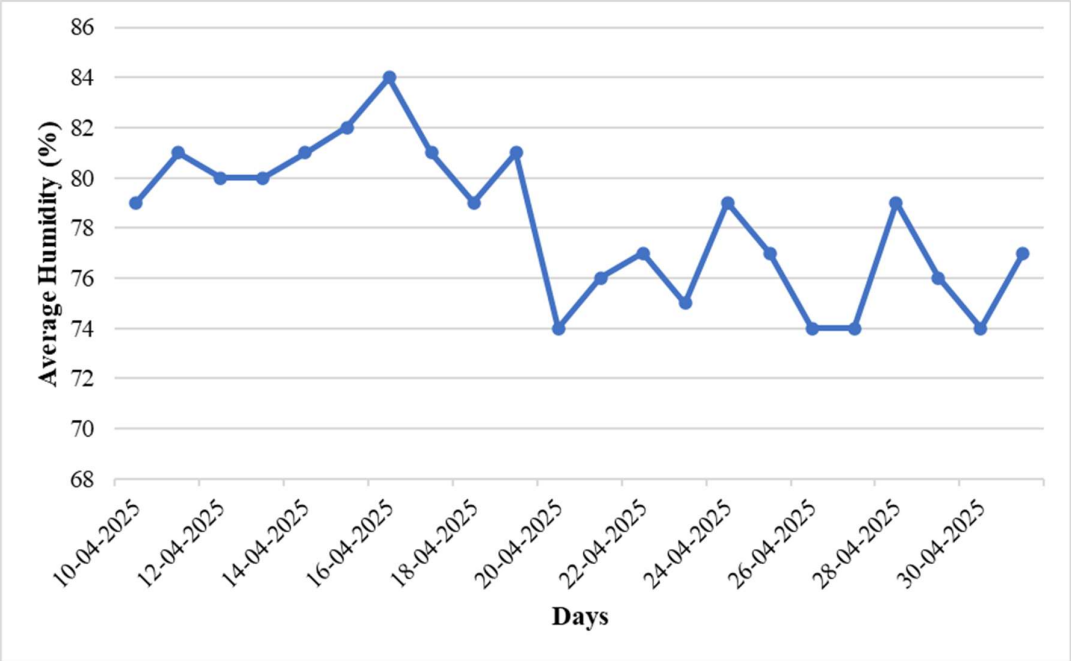


**Fig.4.4 Variation of average relative humidity inside poly house during crop growth period**

4.4 DETERMINATION OF $ET_0$ AND $ET_c$

### 4.4.1 Determination of $ET_0$ using CROPWAT

The reference evapotranspiration ($ET_0$) was estimated using the CROPWAT 8.0 software developed by FAO. The primary climatic input parameters used were the daily minimum and maximum air temperatures, which were recorded using DHT22 sensors installed inside the polyhouse as part of the lysimeter setup. The software processed this data and provided daily $ET_0$ values for the entire crop duration. Table 4.5 gives agro-meteorological parameters and reference evapotranspiration observed during the crop period, which was computed using the CROPWAT software.

**Table.4.5 Agro-meteorological parameters and reference evapotranspiration observed during the crop period**

| S. no | Date | Min Temp (°C) | Max Temp (°C) | Humidity (%) | Wind (Km/day) | Sun Light (hrs) | Rad (MJ/m²/day) | $ET_0$ (mm/day) |
|---|---|---|---|---|---|---|---|---|
| 1 | 10-Apr | 25 | 38.5 | 77 | 173 | 7.2 | 20.7 | 5.56 |
| 2 | 11-Apr | 28.4 | 38.7 | 78 | 173 | 7.1 | 20.5 | 5.52 |
| 3 | 12-Apr | 27.9 | 38.3 | 78 | 173 | 7.3 | 20.8 | 5.5 |
| 4 | 13-Apr | 28 | 38.3 | 78 | 173 | 7.2 | 20.7 | 4.78 |
| 5 | 14-Apr | 28.1 | 36.3 | 82 | 173 | 5.8 | 18.5 | 5.21 |
| 6 | 15-Apr | 28.3 | 37.6 | 80 | 173 | 6.6 | 19.7 | 4.72 |
| 7 | 16-Apr | 28.4 | 36.3 | 82 | 173 | 5.6 | 18.2 | 5.36 |
| 8 | 17-Apr | 28.6 | 38.3 | 79 | 173 | 6.8 | 20 | 5.47 |
| 9 | 18-Apr | 28.3 | 38.4 | 78 | 173 | 7.1 | 20.5 | 5.46 |
| 10 | 19-Apr | 28.2 | 38.3 | 78 | 173 | 7.1 | 20.5 | 6.62 |
| 11 | 20-Apr | 27.5 | 41.3 | 73 | 173 | 9.4 | 24 | 6.23 |
| 12 | 21-Apr | 27.6 | 40 | 75 | 173 | 8.7 | 22.9 | 6.36 |
| 13 | 22-Apr | 28.2 | 40.9 | 75 | 173 | 8.8 | 23.1 | 6.3 |
| 14 | 23-Apr | 28.4 | 40.9 | 75 | 173 | 8.6 | 22.8 | 5.61 |
| 15 | 24-Apr | 27.8 | 38.5 | 77 | 173 | 7.5 | 21.1 | 6.37 |
| 16 | 25-Apr | 26.6 | 40.1 | 74 | 173 | 9.2 | 23.7 | 6.49 |
| 17 | 26-Apr | 26 | 40.1 | 73 | 173 | 9.6 | 24.3 | 5.9 |
| 18 | 27-Apr | 26 | 38.3 | 75 | 173 | 8.5 | 22.6 | 5.8 |
| 19 | 28-Apr | 29 | 39.8 | 77 | 173 | 7.6 | 21.2 | 6.07 |
| 20 | 29-Apr | 27.4 | 39.5 | 75 | 173 | 8.5 | 22.5 | 6.3 |
| 21 | 30-Apr | 26 | 39.5 | 73 | 173 | 9.3 | 23.8 | 5.95 |
| 22 | 01-May | 28 | 39.6 | 76 | 173 | 8.1 | 21.9 | 6.09 |

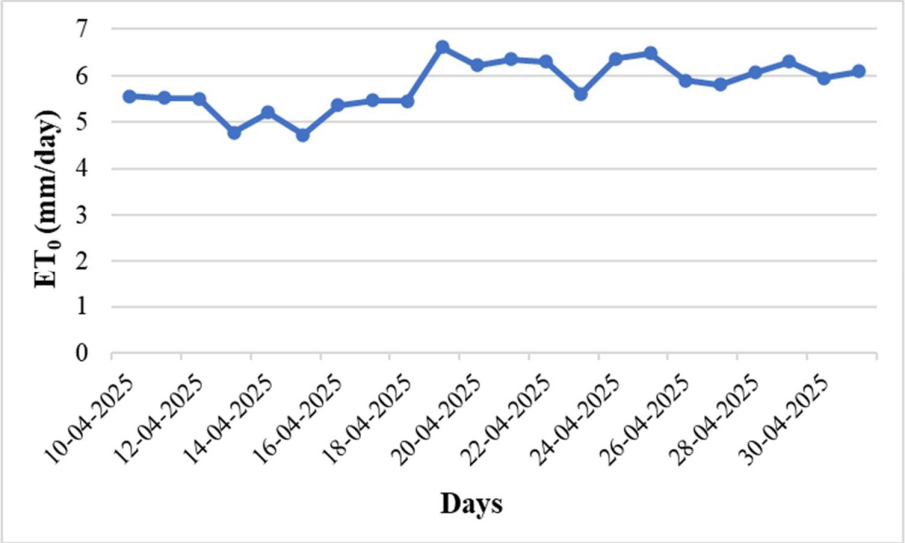


**Fig.4.5 Daily variation of reference crop evapotranspiration inside the polyhouse**

### 4.4.2 Determination of $ET_C$ Using Lysimeter

The actual evapotranspiration ($ET_C$) of *Amaranthus dubius* was meticulously quantified using a smart weighing lysimeter strategically installed within a controlled polyhouse environment. This advanced device continuously recorded changes in the system's weight at 1-hour intervals, effectively capturing the real-time water loss attributed to evapotranspiration throughout the crop's lifecycle. $ET_C$ values were systematically determined by calculating the difference in daily weight between consecutive measurements, incorporating corrections for both irrigation input and any observable drainage. The resultant weight reduction directly mirrored the volume of water transpired by the crop and evaporated from the soil surface, thus providing a reliable estimate of actual water use. This empirical data formed the basis for evaluating the crop's water requirements under polyhouse conditions.

Notably, the data revealed a progressive increase in $ET_C$ immediately following transplanting, beginning at 2.6 mm/day and peaking at 5.91 mm/day, indicating an intensification in plant water uptake as the crop established and developed foliage. This increment is indicative of increased stomatal activity and biomass expansion during the vegetative phase, thereby escalating transpiration rates. However, a pronounced decline was observed post-harvest, with $ET_C$ dropping to 2.07 mm/day, reflecting a substantial reduction in water consumption as the physiological activity of the plants ceased. This

pattern underscores the lysimeter's sensitivity in capturing dynamic evapotranspiration trends and reinforces the importance of stage-wise irrigation planning. The observed values were later juxtaposed with reference evapotranspiration ($ET_0$) to compute the crop coefficient (Kc), which is further elucidated in the subsequent section. Table 4.6 gives details regarding water balance components during the study period inside the polyhouse and crop evapotranspiration of *Amaranthus dubius.* The graphical representation **of the daily variation in actual evapotranspiration for Amaranthus dubius is given in Figure** 4.6.

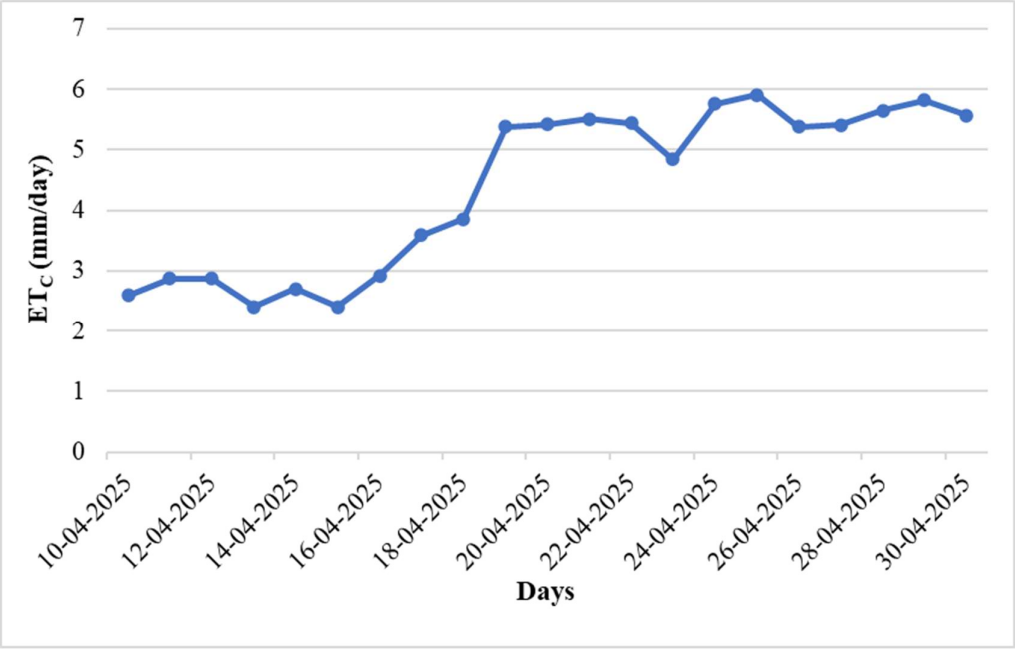


**Fig.4.6 Daily variation of actual evapotranspiration for *Amaranthus dubius***

**Table.4.6 Water balance components and crop evapotranspiration of *Amaranthus dubius***

| Sl. No | Day | Before Watering (Kg) | After Watering(Kg) | Drained Water (Litres) | Water Used by Plant (Kg/day) | Conversion Factor | $ET_c$(mm /day) |
|---|---|---|---|---|---|---|---|
| 1 | 10-Apr | 352.44 | 350.43 | 0.2 | 2.29 | 1.136 | 2.6 |
| 2 | 11-Apr | 347.94 | 354.36 | 0.3 | 2.52 | 1.136 | 2.87 |
| 3 | 12-Apr | 351.52 | 357.57 | 0.32 | 2.53 | 1.136 | 2.87 |
| 4 | 13-Apr | 354.74 | 359.93 | 0.3 | 2.12 | 1.136 | 2.41 |
| 5 | 14-Apr | 357.52 | 362.5 | 0.29 | 2.38 | 1.136 | 2.71 |
| 6 | 15-Apr | 359.85 | 364.64 | 0.27 | 2.12 | 1.136 | 2.41 |
| 7 | 16-Apr | 362.26 | 366.87 | 0.26 | 2.57 | 1.136 | 2.92 |
| 8 | 17-Apr | 364.04 | 368.41 | 0.26 | 3.16 | 1.136 | 3.59 |
| 9 | 18-Apr | 365.01 | 369.14 | 0.24 | 3.4 | 1.136 | 3.86 |
| 10 | 19-Apr | 365.55 | 369.26 | 0.19 | 4.74 | 1.136 | 5.38 |
| 11 | 20-Apr | 364.35 | 367.61 | 0.17 | 4.77 | 1.136 | 5.42 |
| 12 | 21-Apr | 362.73 | 365.07 | 0.11 | 4.85 | 1.136 | 5.51 |
| 13 | 22-Apr | 360.14 | 361.89 | 0.08 | 4.79 | 1.136 | 5.44 |
| 14 | 23-Apr | 356.2 | 357.65 | 0.9 | 4.26 | 1.136 | 4.84 |
| 15 | 24-Apr | 353.28 | 354.68 | 0.11 | 5.07 | 1.136 | 5.76 |
| 16 | 25-Apr | 349.51 | 350.63 | 0.1 | 5.2 | 1.136 | 5.91 |
| 17 | 26-Apr | 345.3 | 346.7 | 0.13 | 4.74 | 1.136 | 5.38 |
| 18 | 27-Apr | 341.83 | 343.42 | 0.13 | 4.76 | 1.136 | 5.41 |
| 19 | 28-Apr | 337.84 | 339.76 | 0.82 | 4.97 | 1.136 | 5.65 |
| 20 | 29-Apr | 334.73 | 337.93 | 0.06 | 5.13 | 1.136 | 5.82 |
| 21 | 30-Apr | 332.75 | 335.38 | 0.06 | 4.91 | 1.136 | 5.57 |
| 22 | 01-May | 330.4 | 332.82 | 0.08 | 1.82 | 1.136 | 2.07 |

## 4.5 ESTIMATION OF CROP COEFFICIENT ($K_C$)

The crop coefficient ($K_C$) is a critical parameter in agronomic water management, representing the ratio of actual crop evapotranspiration ($ET_C$) to reference evapotranspiration ($ET_0$). It serves as an empirical indicator of a crop's specific water use relative to the atmospheric demand, thus aiding in the development of precise irrigation strategies. In the present study, $K_C$ values for *Amaranthus dubius* were derived by juxtaposing the actual evapotranspiration measurements acquired from the smart weighing lysimeter with the reference ET values simulated using the CROPWAT model. This comparative analysis enabled the quantification of water consumption across various phenological stages, offering insights into the dynamic water needs of the crop under polyhouse conditions.

The Kc values were computed distinctly for the initial, mid, and late stages of crop development. A progressive increase in $K_C$ was observed from the initial establishment phase to the peak vegetative stage, corresponding with the expansion of leaf area and intensification of transpiration due to increased stomatal conductance. The coefficient reached a maximum of approximately 0.94 during the mid-growth phase, denoting high water use efficiency at the height of physiological activity. As the crop was harvested the crop coefficient reduced to 0.34, signifying a substantial reduction in evapotranspiration as plant metabolic activity waned. These findings underscore the relevance of stage-specific irrigation scheduling and provide a valuable reference for future cultivation of similar leafy vegetables in protected environments, promoting both resource conservation and optimal yield outcomes.

In contrast, the FAO-56 paper (Allen *et al*., 1998) recommends standard $K_C$ values under open-field conditions for leafy vegetables such as lettuce or spinach, which are morphologically and agronomically similar to Amaranthus. For such crops, the $K_C$ values are typically 0.70 during the initial stage, 1.05 during the mid-season, and 0.95 during the late season. The discrepancy between the two sets of values can be attributed to the controlled microclimatic conditions of the polyhouse. Polyhouse environments generally exhibit reduced wind speed, elevated relative humidity, and moderated solar radiation levels. These factors collectively lower the crop's atmospheric water demand and actual evapotranspiration, thereby resulting in lower $K_C$ values compared to those

observed in open-field conditions as described in FAO-56. The tabulated values of daily evapotranspiration, actual crop evapotranspiration, and crop coefficient during the crop period are given in Table 4.7. **The daily variation of crop coefficient for Amaranthus dubius is graphically represented in Figure 4.7.**

**Table 4.7 Daily reference evapotranspiration ($ET_0$), actual crop evapotranspiration ($ET_C$), and crop coefficient ($K_C$) for *Amaranthus dubius***

| S.no | Day | $ET_C$ | $ET_0$ | $K_C$ |
|---|---|---|---|---|
| 1 | 10-Apr | 2.6 | 5.56 | 0.47 |
| 2 | 11-Apr | 2.87 | 5.52 | 0.52 |
| 3 | 12-Apr | 2.87 | 5.5 | 0.52 |
| 4 | 13-Apr | 2.41 | 4.78 | 0.5 |
| 5 | 14-Apr | 2.71 | 5.21 | 0.52 |
| 6 | 15-Apr | 2.41 | 4.72 | 0.51 |
| 7 | 16-Apr | 2.92 | 5.36 | 0.54 |
| 8 | 17-Apr | 3.59 | 5.47 | 0.66 |
| 9 | 18-Apr | 3.86 | 5.46 | 0.71 |
| 10 | 19-Apr | 5.38 | 6.62 | 0.81 |
| 11 | 20-Apr | 5.42 | 6.23 | 0.87 |
| 12 | 21-Apr | 5.51 | 6.36 | 0.87 |
| 13 | 22-Apr | 5.44 | 6.3 | 0.86 |
| 14 | 23-Apr | 4.84 | 5.61 | 0.86 |
| 15 | 24-Apr | 5.76 | 6.37 | 0.9 |
| 16 | 25-Apr | 5.91 | 6.49 | 0.91 |
| 17 | 26-Apr | 5.38 | 5.9 | 0.91 |
| 18 | 27-Apr | 5.41 | 5.8 | 0.93 |
| 19 | 28-Apr | 5.65 | 6.07 | 0.93 |
| 20 | 29-Apr | 5.82 | 6.3 | 0.92 |
| 21 | 30-Apr | 5.57 | 5.95 | 0.94 |
| 22 | 1-May | 2.07 | 6.09 | 0.34 |

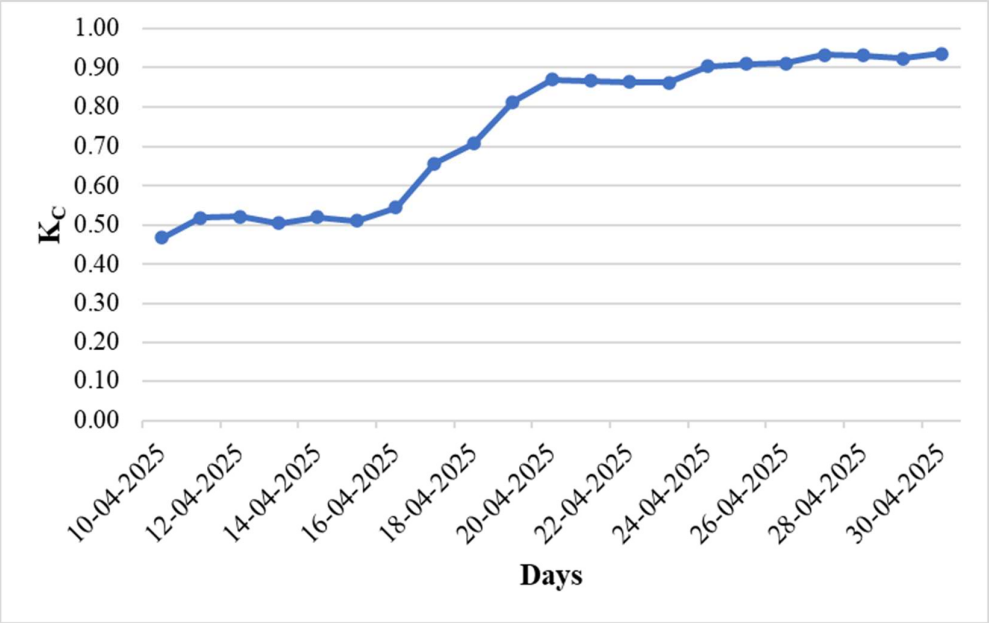


**Fig.4.7 Daily variation of crop coefficient for Amaranthus dubius**

## 4.7 BIOMETRIC OBSERVATIONS OF *Amaranthus dubius*

To assess the vegetative growth and overall performance of *Amaranthus dubius* under polyhouse conditions, detailed biometric observations were systematically conducted. Three representative plants were randomly selected from the total population of 28 plants cultivated inside the protected structure. Key growth parameters recorded included plant height and the number of leaves per plant both reliable indicators of vegetative vigour and physiological development.

In addition to general sampling, focused biometric measurements were also carried out on the three *Amaranthus dubius* plants grown specifically within the lysimeter unit. These plants were monitored more closely, as they were central to the evapotranspiration analysis. Here, a broader range in growth was observed. The average plant height spanned from 12.7 cm during the early establishment phase to a maximum of 68.67 cm at maturity. Similarly, the number of leaves per plant ranged from 8 to 19, highlighting a robust vegetative build-up over time. These variations not only reflect the dynamic growth trajectory of the crop but also serve as a valuable reference when correlating biometric data with actual water use (ET) patterns. Such integrative monitoring supports more precise irrigation scheduling, contributing to efficient resource use and enhanced crop productivity under protected cultivation systems. This

result in height and number of leaves was also obtained in study done by Toyin *et al*., 2015, on Greenhouse evapotranspiration and crop factor of *Amaranthus cruentus* grown in weighing lysimeters. Average height of Amarathus with respect to days after planting is given as tabulated form in table 4.8 along with the heights of selected plants and the graphical representation of average height with respect to days after planting is given in figure 4.8. The number of leaves of the selected plants and their average value is tabulated in table 4.9 and the graphical representation of average number of leaves after planting is given in figure 4.9.

**Table.4.8 Average height of the Amaranthus with respect to days after planting**

| No Of Days After Planting | P1 | P2 | P3 | Average Height |
|---|---|---|---|---|
| 2 | 13.6 | 9.5 | 15 | 12.70 |
| 3 | 13.6 | 9.5 | 15 | 12.70 |
| 4 | 13.8 | 9.7 | 15.9 | 13.13 |
| 5 | 13.9 | 10 | 16 | 13.30 |
| 6 | 14.3 | 10.7 | 16.8 | 13.93 |
| 7 | 15 | 11.8 | 17 | 14.60 |
| 8 | 16.5 | 13 | 19 | 16.17 |
| 9 | 16.8 | 17 | 22 | 18.60 |
| 10 | 17.7 | 19 | 25 | 20.57 |
| 11 | 18.5 | 21 | 28 | 22.50 |
| 12 | 19.1 | 25 | 30 | 24.70 |
| 13 | 21.5 | 29 | 34 | 28.17 |
| 14 | 36 | 31 | 39 | 35.33 |
| 15 | 41 | 36 | 43 | 40.00 |
| 16 | 46.5 | 41 | 47 | 44.83 |
| 17 | 49 | 45.5 | 52 | 48.83 |
| 18 | 50 | 50 | 57.4 | 52.47 |
| 19 | 52 | 53 | 63 | 56.00 |
| 20 | 59.5 | 59 | 66 | 61.50 |
| 21 | 61 | 61.5 | 71 | 64.50 |
| 22 | 63 | 67 | 76 | 68.67 |

**Table.4.9 Number of leaves of the Amaranthus with respect to days after planting**

| No Of Days After Planting | P1 | P2 | P3 | Average |
|---|---|---|---|---|
| 2 | 7 | 6 | 10 | 8 |
| 3 | 7 | 6 | 10 | 8 |
| 4 | 7 | 6 | 10 | 8 |
| 5 | 7 | 7 | 11 | 8 |
| 6 | 7 | 7 | 11 | 8 |
| 7 | 8 | 7 | 12 | 9 |
| 8 | 8 | 8 | 12 | 9 |
| 9 | 9 | 8 | 12 | 10 |
| 10 | 9 | 9 | 12 | 10 |
| 11 | 11 | 9 | 13 | 11 |
| 12 | 11 | 9 | 13 | 11 |
| 13 | 12 | 10 | 15 | 12 |
| 14 | 12 | 10 | 15 | 12 |
| 15 | 12 | 10 | 15 | 12 |
| 16 | 11 | 11 | 16 | 13 |
| 17 | 11 | 12 | 16 | 13 |
| 18 | 14 | 12 | 19 | 15 |
| 19 | 14 | 12 | 21 | 16 |
| 20 | 13 | 13 | 21 | 16 |
| 21 | 14 | 14 | 21 | 16 |
| 22 | 15 | 17 | 24 | 19 |

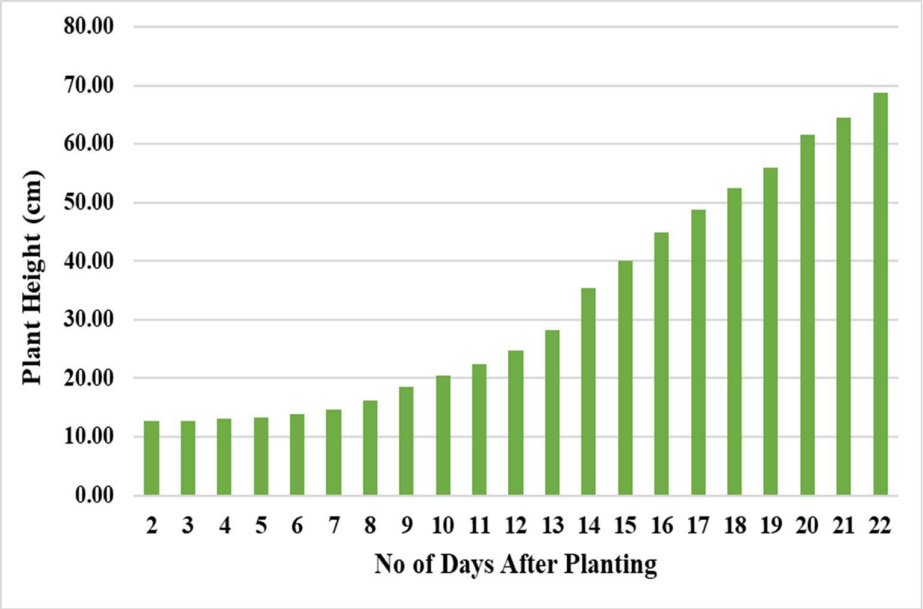


**Fig.4.8 Variation in plant height of Amaranthus with respect to days after planting**

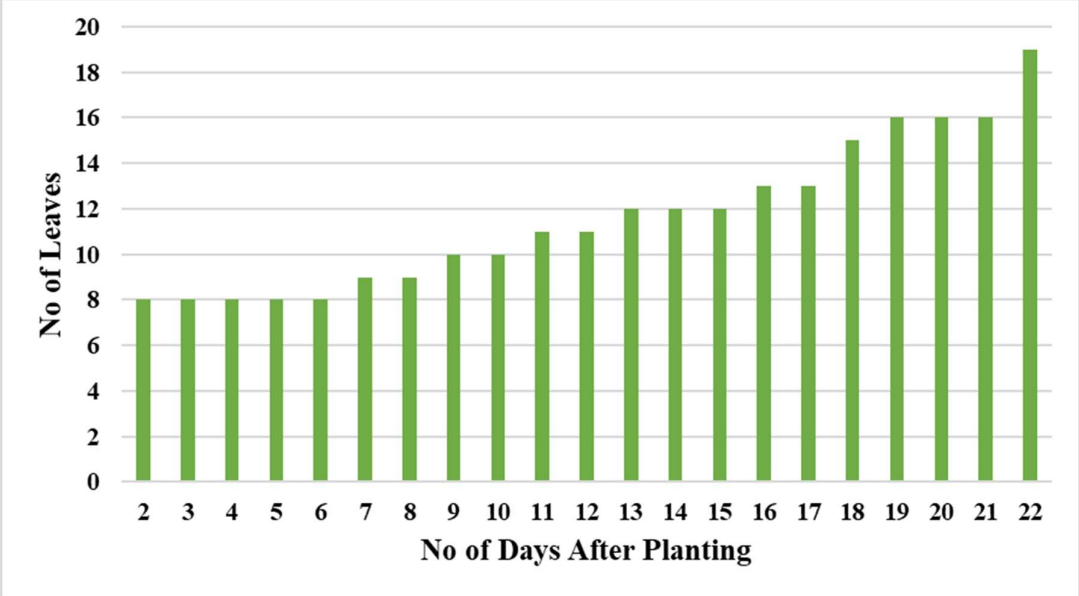


**Fig.4.9 Variation in number of leaves of Amaranthus with respect to days after planting**

## 4.8 YIELD OF *Amaranthus dubius*

The first harvest of *Amaranthus dubius* was conducted on 31st March 2025. A total fresh yield of 1.07 kg was obtained from 28 plants cultivated within the smart weighing lysimeter, which occupied a confined area of 110 cm × 80 cm. This lysimeter unit, along with the surrounding cultivation area, was located within a polyhouse environment, ensuring uniform climatic conditions. In contrast, the surrounding cultivated area, extending to approximately 3 $m^2$, produced a total yield of 2.62 kg. Both areas were subjected to similar agronomic and environmental conditions, allowing a meaningful comparison of crop response within and outside the lysimeter setup. This observation contributes to understanding the performance of *Amaranthus dubius* under controlled polyhouse conditions and highlights the crop's fresh biomass potential in different spatial arrangements.

Although only one harvest was carried out, the yield performance demonstrates the potential of *Amaranthus dubius* under controlled environment agriculture. Further harvesting cycles or replication of the experiment would be useful to confirm consistency and evaluate cumulative yield over time.

# *Summary and conclusion*

# CHAPTER 5

# SUMMARY AND CONCLUSION

The present study was undertaken to design, develop, and evaluate a smart weighing lysimeter for estimating actual evapotranspiration ($ET_C$) and deriving crop coefficient (Kc) values for *Amaranthus dubius* cultivated under polyhouse conditions. The fabricated lysimeter system was integrated with four 300 kg CZL-type load cells, signal amplifiers (HX711), an Arduino Mega 2560 controller, DHT22 temperature and humidity sensor, and a microSD card module for data logging. The system was calibrated and tested within a naturally ventilated polyhouse located at KCAEFT, Tavanur. The experimental crop, *Amaranthus dubius* (Coimbatore Co.1), was monitored throughout its crop cycle. $ET_C$ was measured using the soil water balance method based on lysimeter weight variations, while $ET_0$ was computed using the Penman–Monteith method in the CROPWAT model. Crop coefficient (Kc) values were determined based on the observed $ET_C$ and $ET_0$ data.

- The maximum temperature of 41.3 °C and minimum temperature of 27.4 °C were noted during the crop growth period, the average temperatures ranged between 32.15°C to 34.65°C.
- The average relative humidity within the polyhouse environment was observed to range between 74% and 84%.
- Actual evapotranspiration ($ET_C$) ranged from 2.6 to 5.91 mm/day.
- Reference evapotranspiration ranged from 4.72 to 6.62 mm/day.
- The crop coefficient ($K_C$) was 0.5 during the initial stage, 0.76 during mid-stage, 0.92 during late stage, and dropped to 0.34 after-harvest.
- Fresh yield from the lysimeter plot was 1.07 kg.
- The average height of the plant ranged from 12.7 cm after transplanting to 68.67 cm just before harvesting.
- Average number of leaves per plant ranged from 8 to a maximum of 19.

The developed smart weighing lysimeter proved to be a cost-effective and efficient tool for precise, real-time estimation of actual evapotranspiration and

monitoring of soil-plant-water interactions. The peak $K_C$ during the mid-stage to pre-harvesting period underscores the importance of increased water demand during vigorous vegetative growth. Overall, the lysimeter-based $ET_C$ measurements and derived $K_C$ values can significantly enhance water use efficiency and promote sustainable irrigation practices, especially for leafy vegetables like *Amaranthus dubius* grown under polyhouse conditions.

# *References*

## REFERENCES


Abedinpour, M. 2015. Evaluation of growth-stage-specific crop coefficients of maize using weighing lysimeter. *Soil and Water Res.* 10(2): 99-104.

Abhiram, G., McCurdy, M., Davies, C.E., Grafton, M., Jeyakumar, P., and Bishop, P. 2023. An innovative lysimeter system for controlled climate studies. *Biosystems Eng.* 228: 105-119.

Aboukhaled, A., Alfaro, A. and Smith, M. 1982. Lysimeters. In: Food and Agriculture Organization of United Nations. *FAO Irrigation and Drainage Paper 39*. Rome, Italy. Food and Agriculture Organization of United Nations, Italy.

Ahmed, F.K. 1991. Measuring actual evapotranspiration from sweet corn with lysimeters in a semi-arid region. Ph.D. dissertation, Utah State University, 0p.

Allen, R.G., Pereira, L.S., Raes, D., and Smith, M. 1998. *Crop Evapotranspiration – Guidelines for Computing Crop Water Requirements*. FAO, Rome, 300p.

Allen, R.G., Smith, M., Perrier, A., and Pereira, L.S. 1994. An update for the definition of reference evapotranspiration. *ICID Bull. 43*(2): 1-34.

Allen, R.G., Howell, T.A., Pruitt, W.O., Walter, I.A. and Jensen, M.E. 1991. Lysimeters for evapotranspiration and environmental measurements. In: Proceedings of the International Symposium on Lysimetry, *ASCE*, New York. ASCE, New York, pp. 456.

Burman, R.D., Cuenca, R.H. and Weiss, A. 1983. Techniques for estimating irrigation water requirements. In: Hillel, D. (ed.), *Advances in Irrigation*. Academic Press, New York, pp. 335-393.

Challa, L.P., Singh, C.D., Rao, K.V., and Kumar, M. 2022. Micro-Climatic Variations in Naturally Ventilated Polyhouse Under Cucumber Cultivation. *Indian J. Ecol. 49*(6): 2194-2201.

Doležal, F., Hernandez-Gomis, R., Matula, S., Gulamov, M., Miháliková, M., and., Khodjaev, S. 2018. Actual evapotranspiration of unirrigated grass in a smart field lysimeter. *Vadose Zone J.* 17(1): 170-173

Dong, Y., and Hansen, H. 2023. Development and design of an affordable field scale weighing lysimeter using a microcontroller system. *Smart Agric. Technol. 4*: 100147.

Dreibelbis, F.R., and Amerman, C.R. 1964. Land use, soil type, and practice effects on the water budget. *J. Geophys. Res. 69*(16): 3387-3393.

Drema, L., Gautam, S., and Rawat, S. 2024. Climatic trends and its impact on reference evapotranspiration and crop water requirement of rice crop in Arunachal Pradesh, India. *J. Agrometeorol. 26*(2): 220-224.

Du Plessis A. 2017. *Freshwater challenges of South Africa and its Upper Vaal River*. Springer, Berlin, Germany: 129–151.

Ekern, P. C. 1965. Evapotranspiration of pineapple in Hawaii. *Plant Physiol*. 40: 736-739

FAO. 1992. Report of the expert consultation on procedures for revision of FAO guidelines for prediction of crop water requirements. In: UN-FAO. (ed.), *Report of the Expert Consultation*. UN-FAO, Rome, Italy. UN-FAO, Rome, pp. 54.

Farzaneh Zardoshti, F., Bakhtiari, B., Qaderi, K., Khanjani, M.J., Banayan, M. 2018. Design and construction of a portable smart weighing lysimeter for accurate measurement of crop water requirement. *Iranian J. Soil Water Res*. 49: 695–704.

Feng, Z., Liu, D. and Zhang, Y. 2007. Water requirements and irrigation scheduling of spring maize using GIS and CROPWAT model in Beijing-Tianjin-Hebei region. *Chinese Geographical Science*, 17(1): 56–63.

Fritschen, L. J., and C. H. M. van Bavel. 1964. Energy balance as affected by height and maturity of sudangrass. *Agron. J*. 56: 201-204.

Gale, J. 1961. Studies on plant antitranspirants. *Plant Physiol*. 14: 777-786

Gao, Z., Yang, D., Li, C., Zhang, J., and Wang, Q., 2025. A review of lysimeters from the perspective of measurement performance and intelligent development in China. *Irrig. Drain. 74*(1): 276-298.

George, B.A., Shende, S.A. and Raghuwanshi, N.S. 2000. Development and testing of an irrigation scheduling model. *Agricultural Water Management*, 46(2): 121–136.

Gonzalez, F., Pavek, M.J., Holden, Z.J. and Garza, R., 2023. Evaluating potato evapotranspiration and crop coefficients in the Columbia Basin of Washington state. *Agric. Water Manage.*, 286: 108371.

Guerra E., Ventura F. and Snyder R.L. 2016. Crop coefficients: A literature review. *J. Irrig. Drain. Eng.* 142(3): 601-5006.

Gupta, D., Santosh, D.T., and Debnath, S. 2020. Modeling and simulation a: lication for greenhouse microclimatic studies and structural analysis. *Protected Cultivation Smart Agric.*: 300-312.

Haise, H. R., Hanks, R. J., and M. E. Jensen. 1963. Solar reflection from various crops and conditions. *Agron. Abstr.* p. 7

Hargreaves, G.H. 1989. Accuracy of estimated reference crop evapotranspiration. *J. Irrig. Drain. Eng. 115*(6): 1000-1007.

Hargreaves, G.H. 1994. Defining and using reference evapotranspiration. *J. Irrig. Drain. Eng. 120*(6): 1132-1139.

Howell, T.A., Schneider, A.D. and Jensen, M.E., 1991. History of lysimeter design and use for evapotranspiration measurements. *Lysimeters for evapotranspiration and environ. Measurements*: 1-9.

Irmak, S. 2009. Estimating Crop Evapotranspiration from Reference Evapotranspiration and Crop coefficients. *Univ. Neb-Lincol J:* 1 – 12.

Jain R., Kishore P. and Singh D.K. 2019. Irrigation in India: Status, challenges and options. *J. Soil Water Conserv*. 18(4): 354–363

Jiménez-Carvajal, C., Ruiz-Peñalver, L., Vera-Repullo, J.A., Jiménez-Buendía, M., Antolino-Merino, A. and Molina-Martínez, J.M. 2017. Weighing lysimetric system for the determination of the water balance during irrigation in potted plants. *Agric. water manag. 183:* 78-85.

Kashyap, P.S. and Panda, R.K. 2001. Evaluation of evapotranspiration estimation methods and development of crop-coefficients for rice under a sub-humid region. *Agric. Water Manage.* 50(1): 9–25.

Kebede, N., Ayana, M., Mekonnen, B. and Beri, H. 2024. Design, construction, and calibration of a weighable lysimeter for measuring water requirements of field crops for data-scarce areas of Ethiopia. *Heliyon*. 10(17): 36968

Kolapkar, M.M. and Sayyad, S.B. 2020. Greenhouse microclimate study for humidity, temperature and soil moisture using agricultural wireless sensor network system. In: *International Conference on Recent Trends in Image Processing and Pattern Recognition*. Singapore. Springer Singapore, Singapore, pp. 278-289.

Kumar, A., and Kumar, P. 2012. Estimation of evapotranspiration using lysimeter and climatic data. *Agric. Water Manag.* 108: 31–37.

Kumar, R., Jat, M.K. and Shankar, V. 2012. Methods to estimate irrigated reference crop evapotranspiration–a review. *Water Sci. Tehnol. 66*(3): 525-535.

Kumari, N., Srivastava, A. 2020. An approach for estimation of evapotranspiration by standardizing parsimonious method. *Agric. Res*. 9: 301–309.

Lemon, E.R., Glaser, A.H., and Satterwhite, L.E. 1957. Some aspects of the relationship of soil, plant, and meteorological factors to evapotranspiration. In: Soil Science Society of America (ed.), *Proceedings of the Soil Science Society of America*. pp.464-468.

López-Urrea, R., Pardo, J.J., Simón, L., Martínez-Romero, Á., Montoya, F., Tarjuelo, J.M. and Domínguez, A. 2021. Assessing a removable mini-lysimeter for monitoring crop evapotranspiration using a well-established large weighing lysimeter: a case study for barley and potato. *Agron.*, 11(10): 2067.

MA Abd El-Bary, W., M Hegazi, M., F El-Bagoury, K., M Sultan, W. and M Mubarak, M. 2022. Modification Of Microclimate Conditions For Improving Tomato Plant Growth Components And Water Use Efficiency. *Misr J. Agric. Eng. 39*(1): 119-132.

Madhavi, T. 2017. Comparative evaluation of evapotranspiration parameters in a naturally ventilated polyhouse and open field. Doctoral dissertation, Kelappadji College of Agricultural Engineering and Technology, Tavanur, 139p

Malone, R.W., Bonta, J.V., Stewardson, D.J. and., Nelsen, T., 2000. Error analysis and quality improvement of the Coshocton weighing lysimeters. *Trans. of the ASAE*. *43*(2): 271-280.

Marek, T., Piccinni, G., Schneider, A., Howell, T., Jett, M. and Dusek, D.J.A.E.I.A. 2006. Weighing lysimeters for the determination of crop water requirements and crop coefficients. *Appl. Eng. Agri*. *22*(6): 851-856.

Marlatt, W.E., 1961. *The interactions of microclimate, plant cover, and soil moisture content affecting evapotranspiration rates* (No. 23). Colorado State University, Department of Atmospheric Science.

Meena, K., Sharma, R. and Patel, P. 2021. Lysimeter-based measurement of evapotranspiration under different irrigation systems. *Irrig. Sci.* 39(5): 461–474.

Meissner, R., Prasad, M.N.V. and Rinklebe, J. 2010. Lysimeter application for measuring the water and solute fluxes with high precision. *Curr. Sci.* 99(5)

Monteith, J.L., 1959. The reflection of short-wave radiation by vegetation. *Quarterly J. R. Meteorological Soc. 85*(366): 386-392.

Nicolás-Cuevas, J.A., Parras-Burgos, D., Soler-Méndez, M., Ruiz-Canales, A., and Molina-Martínez, J.M. 2020. Removable weighing lysimeter for use in horticultural crops. *A: lied Sci. 10*(14): 4865.

Niranjan, S., and Nandagiri, L. 2024. Development of daily gridded Penman-Monteith reference crop evapotranspiration data for Karnataka State, India. *ISH J. Hydraulic Eng. 30*(1): 85-99.

Oliveira, G., Almeida, C., Santos, J.M., Martins, J.C., and Jasnau Caeiro, J. 2022. IoT lysimeter system with enhanced data security. In: *APCA International Conference on Automatic Control and Soft Computing*. APCA International Conference on Automatic Control and Soft Computing, Cham. Springer International Publishing, Cham, pp. 119-129.

Pandey, S., and Pandey, D. 2011. Application of lysimeter for crop evapotranspiration studies. *Irrig. Drain. Syst.* 25(4): 225–233.

Penman, H.L. 1956. Evaporation: An introductory survey. *Neth. J. Agric. Science*, 4: 9–29.

Pereira, L.S., Paredes, P., Melton, F., Johnson, L., Mota, M. and Wang, T., 2021. Prediction of crop coefficients from fraction of ground cover and height: Practical application to vegetable, field and fruit crops with focus on parameterization. *Agric. Water Manage.* 252: 106663.

Rahil M.H. and Qanadillo A. 2015. Effects of different irrigation regimes on yield and water use efficiency of cucumber crop. *Agric. Water Manag.* 148: 10–15.

Rajput, J., Singh, M., Lal, K., Khanna, M., Sarangi, A., Mukherjee, J., Singh, S., and Dimple. 2024. Development of single and dual crop coefficients for drip-irrigated broccoli using weighing type field lysimeters in semi-arid environment. *Environ. Dev. Sustainability*: 1-27.

Rana G., Katerji N., Mastrorilli M. and El Moujabber M. (1994). Evapotranspiration and canopy resistance of grass in a Mediterranean region. *Theor. Appl. Climatol.* 50: 61–71.

Reddy, G.V., Ayyanagoudar, M.S., Babu, B.M., Ajayakumar, M.Y., and Meena, M.K., 2023. Determination of crop water requirement and crop coefficient at different growth stages of tomato by using weighing type lysimeter in raichur region. *Int. J. Environ. Clim. Change*, *13*(8): 964-972.

Ridder, N.A., and Boonstra, J. 1994. Analysis of water balances. In: Ritzema, H.P. (2nd), *Drainage Principles and Applications*. ILRI, Netherlands. ILRI, Netherlands, pp. 601-633.

Romashchenko, M., Shatkowski, A., and Zhuravlev, O. 2016. Features of application of the Penman–Monteith method for conditions of drip irrigation in the steppe of Ukraine. *J. Water Land Dev.* 31(1): 123–127.

Sagar, A., Hasan, M., Singh, D.K., Al-Ansari, N., Chakraborty, D., Singh, M.C., Iquebal, M.A., Kumar, A., Malkani, P., Vishwakarma, D.K. and Elbeltagi, A. 2022. Development of smart weighing lysimeter for measuring evapotranspiration and developing crop coefficient for greenhouse chrysanthemum. *Sensors*, 22(16): 62-39.

Santosh, D.T. 2021. Response of horticultural crops under variable microclimatic conditions of different protected cultivation structures. *Int. J. Agric. Sci.* 17(2): 515-521

Sarma, A. and Bharadwaj, K. 2020. Determination of crop coefficients and estimation of evapotranspiration of rapeseed using lysimeter and different reference evapotranspiration models. *J. Agrometeorol.* 22(2): 172–178.

Schmidt, B., 2022. Smart Lysimeter: An Autonomous, Low-Cost, And Portable Lysimeter For Use In A Greenhouse.

Schneider, A.D., Howell, T.A., Moustafa, A.T.A., Evett, S.R. and Abou-Zeid, W. 1998. A simplified weighing lysimeter for monolithic or reconstructed soils. *Appl. Eng. in Agric. 14*(3): 267-273.

Schrader, S., Zanzot, J., and Miller, T. 2023. Application of lysimeter data for regional evapotranspiration estimation and irrigation optimization. *Water Resour. Manag.* 37(6): 237–249.

Shi, W., Zhang, X., Xue, X., Feng, F., Zheng, W., and Chen, L. 2023. Analyzing Evapotranspiration in Greenhouses: A Lysimeter-Based Calculation and Evaluation Approach. *Agron.*, *13*(12): 3059.

Smith, M. 1992. CROPWAT*:* A computer program for irrigation planning and management*. Food Agric. Org*. 46: 133.

Sojitra, M.A., Satasiya, R.M., Rank, H.D., Chauhan, P.M., Parmar, H.V., and Patel, D.V. 2023. Study the micro climatic parameter in protected structure. *Environ. Ecol*. 41 (2A): 953-960

Stöckle, C.O., Liu, M., Kadam, S.A., Evett, S.R., Marek, G.W., and Colaizzi, P.D. 2025. Comparing evapotranspiration estimations using crop model-data fusion and

satellite data-based models with lysimetric observations: Implications for irrigation scheduling. *Agric. Water Manag. 311*: 109372.

Surendran, U., Sushanth, C.M., Mammen, G. and Joseph, E.J. 2015. Modelling the crop water requirement using FAO-CROPWAT and assessment of water resources for sustainable water resource management: A case study in Palakkad district, Kerala. *Aquatic Procedia*, 4: 1211–1219.

Tabari, H. 2010. Evaluation of reference crop evapotranspiration equations in various climates. *Water Resour. Manag. 24*: 2311-2337.

Talebmorad, H., Abedi-Koupai, J., Eslamian, S., Mousavi, S.F., Akhavan, S., Ostad-Ali-Askari, K., and Singh, V.P. 2021. Evaluation of the impact of climate change on reference crop evapotranspiration in Hamedan-Bahar plain. *Int. J. Hydrol. Sci. Tehnol. 11*(3): 333-347.

Tanner, C.B., and Lemon, E.R. 1962. Radiant energy utilization and evapotranspiration in a bean canopy. *Agron. J.* 54(4): 329–334.

Tanner, C.B., Sinclair, T.R., and Lemon, E.R. 1960. Evaporation of corn at different plant populations. *Agron. J.* 52(6): 330–333.

Toyin, F.J., Miguel, R.J., Gbenro, O.P. and Ebenezer, A.A. 2015. Greenhouse evapotranspiration and crop factor of *Amaranthus cruentus* grown in weighing lysimeters. *Afr. J. Agric. Res.*, 10(34): 3453–3461.

Tyagi, N.; Sharma, D.; Luthra, S. 2000. Determination of evapotranspiration and crop coefficients of rice and sunflower with lysimeter. *Agric. Water Manag.* 45: 41–54.

Van Bavel, C.H.M., and Wilson, D.R. 1952. Soil water depletion and evapotranspiration by irrigated alfalfa and grass. *Agron. J.*, 44(1):3–8.

Viets, F.G. 1962. Fertilizers and the efficient use of water. *Adv. Agron.* 14: 223–264.

Villalobos F.J., Testi L. and Fereres E. 2017. Calculation of evapotranspiration and crop water requirements. *In: Principles of Agron. for Sustain. Agric*: 119–137.

Vozhehova, R.A., Lavrynenko, Y.O., Kokovikhin, S.V., Lykhovyd, P.V .2018. Assessment of the CROPWAT 8.0 software reliability for evapotranspiration and crop water requirements calculations. *J. Water Land Dev*. 39: 147–152.

Yang, S., Aydin, M., Yano, T., and., Li, X. 2003. Evapotranspiration of orange trees in greenhouse lysimeters. *Irrig. Sci.21* :145-149.

Zelitch, I. 1964. The control of stomatal opening. *Annu. Rev. Plant Physiol.* 15: 329–346.

Zhuravlev, O.V. 2016. Peculiarities of Penman-Monteith method use in conditions of drip irrigation in Ukraine. In: *Drip Irrigation and Intensive Agrotechnologies of the XXI Century* :39–43.

Zupanc, V., Zeleznik, B.B., and Pintar, M. 2005. Water balance assessment for lysimeter station based on Water Pumping Station Kleče in Ljubljana. *Acta Agric. Slovenica*. 85(1): 83 – 90

# APPENDIX I

## Physical properties of soil by Core cutter method

**Calculations**

Weight of core soil (W) : 1642.2 g

Volume of core soil (V) : 966 $cm^3$

Weight of moisture container ($W_1$) : 334.5 g

Weight of moist soil + Moisture container weight ($W_2$) : 1976.65 g

Weight of dry soil + Moisture container weight ($W_3$) : 1863.5 g

Moisture content of soil (ω) : 7.4%

Bulk density and particle density of soil were determined by using the following formulas

Bulk density of the soil ($g/cm^3$) $\gamma = \frac{W}{V}$

= 1642.2/966

= 1.7 g/cc

Dry density of the soil ($g/cm^3$) $\gamma_d = \frac{\gamma}{1+\omega}$

= 1.7/ (1+0.074)

= 1.58 g/cc

## APPENDIX II

### Conversion Factor for Calibration of Loadcell

Density of water = 1000 kg/$m^3$

= 1 kg/L

Weight of water = 1 kg

Density = $\frac{Mass}{Volume}$

Volume = $\frac{1\ Kg}{1\ Kg/L}$ = 1L

But, 1L = $10^6$ $mm^3$

Dimension of Lysimeter = 110 cm × 80 cm × 60 cm

Area of Lysimeter tank = 110 × 80 $cm^2$ = 8800 $cm^2$ = 0.88 $m^2$ = 0.88 × $10^6$ $mm^2$

Amount of water lost in mm = $\frac{Volume}{Area}$ = $10^6$ $mm^3$/ 0.88 × $10^6$ $mm^2$

= 1.136

# DESIGN AND DEVELOPMENT OF SMART WEIGHING LYSIMETER FOR EVAPOTRANSPIRATION STUDIES

**BY**

**DHAKSHINA DEVADASAN (2021-02-001)**

**ASHIKA N (2021-02-013)**

**AKSA ELIZABETH JOSE (2021-02-015)**

## ABSTRACT

Submitted in partial fulfilment of the requirement for the degree of

***BACHELOR OF TECHNOLOGY IN AGRICULTURAL ENGINEERING***

**Faculty of Agricultural Engineering and Technology**


**Kerala Agricultural University**

**DEPARTMENT OF IRRIGATION AND DRAINAGE ENGINEERING**

**KELAPPAJI COLLEGE OF AGRICULTURAL ENGINEERING AND FOOD TECHNOLOGY**

**Tavanur-679573, Malappuram**

**Kerala, India**

**2025**

## ABSTRACT

Accurate estimation of crop evapotranspiration ($ET_C$) is vital for efficient irrigation scheduling and sustainable water resource management, particularly in regions facing water scarcity. This study focused on the design and development of a cost-effective smart weighing lysimeter to determine the actual evapotranspiration ($ET_C$) and crop coefficient ($K_C$) of *Amaranthus dubius* under polyhouse conditions. The lysimeter comprised a modified tank (110 × 80 × 60 cm) supported by four CZL-642 300 kg load cells arranged in a rectangular configuration. These load cells were interfaced with HX711 amplifiers and an Arduino Mega 2560 microcontroller to enable continuous weight monitoring. For environmental monitoring, a DHT22 sensor was integrated to record temperature and relative humidity. Data was logged on an SD card via a real-time clock (RTC) module at one-minute intervals.

The experiment was conducted within a naturally ventilated polyhouse at KCAEFT, Tavanur, Kerala. Throughout the crop lifecycle, the system recorded weight variations and environmental parameters, which were used to compute $ET_C$ and derive stage-wise $K_C$ values for *Amaranthus dubius*. The $ET_C$ values were validated against reference evapotranspiration ($ET_0$) computed using the FAO Penman–Monteith method through CROPWAT 8.0 software. The crop coefficient values varied with growth stages, peaking during the mid-season phase.

The developed smart lysimeter demonstrated high precision, minimal calibration error, and consistent performance, confirming its reliability. Its affordability, simplicity, and accuracy make it a valuable tool for researchers and farmers to improve irrigation scheduling and water productivity. This study highlights the potential of integrating low-cost electronics with open-source platforms for real-time monitoring of evapotranspiration, thereby supporting localized and data-driven irrigation strategies in protected cultivation systems.